



NASA CR-159,113

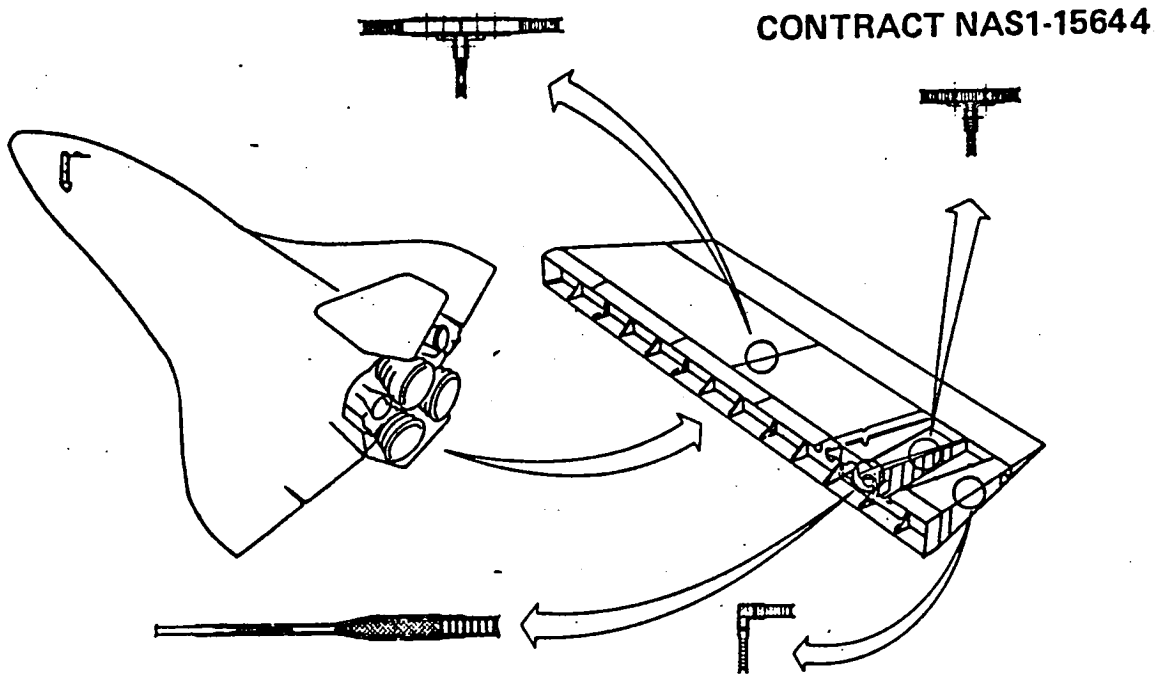
NASA Contractor Report Number 159113

DESIGN, FABRICATION AND TEST OF GRAPHITE/POLYIMIDE COMPOSITE JOINTS AND ATTACHMENTS FOR ADVANCED AEROSPACE VEHICLES

QUARTERLY TECHNICAL PROGRESS REPORT NO. 6
COVERING THE PERIOD FROM

MAY 1, 1980 Through NOVEMBER 30, 1980

NASA-CR-159113
19810016606



CONTRACT NAS1-15644

PREPARED FOR
NATIONAL AERONAUTICS AND SPACE ADMINISTRATION
LANGLEY RESEARCH CENTER
HAMPTON, VIRGINIA 23665

December 15, 1980

BOEING AEROSPACE COMPANY
ENGINEERING TECHNOLOGY
POST OFFICE BOX 3999
SEATTLE, WASHINGTON 98124

MAY 15



FOREWORD

This report summarizes the work performed by the Boeing Aerospace Company (BAC) under NASA Contract NAS1-15644 during the period May 1, 1980, through November 30, 1980.

This program is sponsored by the National Aeronautics and Space Administration, Langley Research Center (NASA/LaRC), Hampton, Virginia. Dr. Paul A. Cooper is the Technical Representative for NASA/LaRC.

Performance of this contract is by Engineering Technology personnel of BAC. Mr. J. E. Harrison is the Program Manager and Mr. D. E. Skoumal is the Technical Leader.

The following Boeing personnel were principal contributors to the program during this reporting period: D. L. Barclay, Design; J. B. Cushman, Analysis; S. G. Hill, Materials and Processes; and S. M. Williams, Finite Element Analysis.

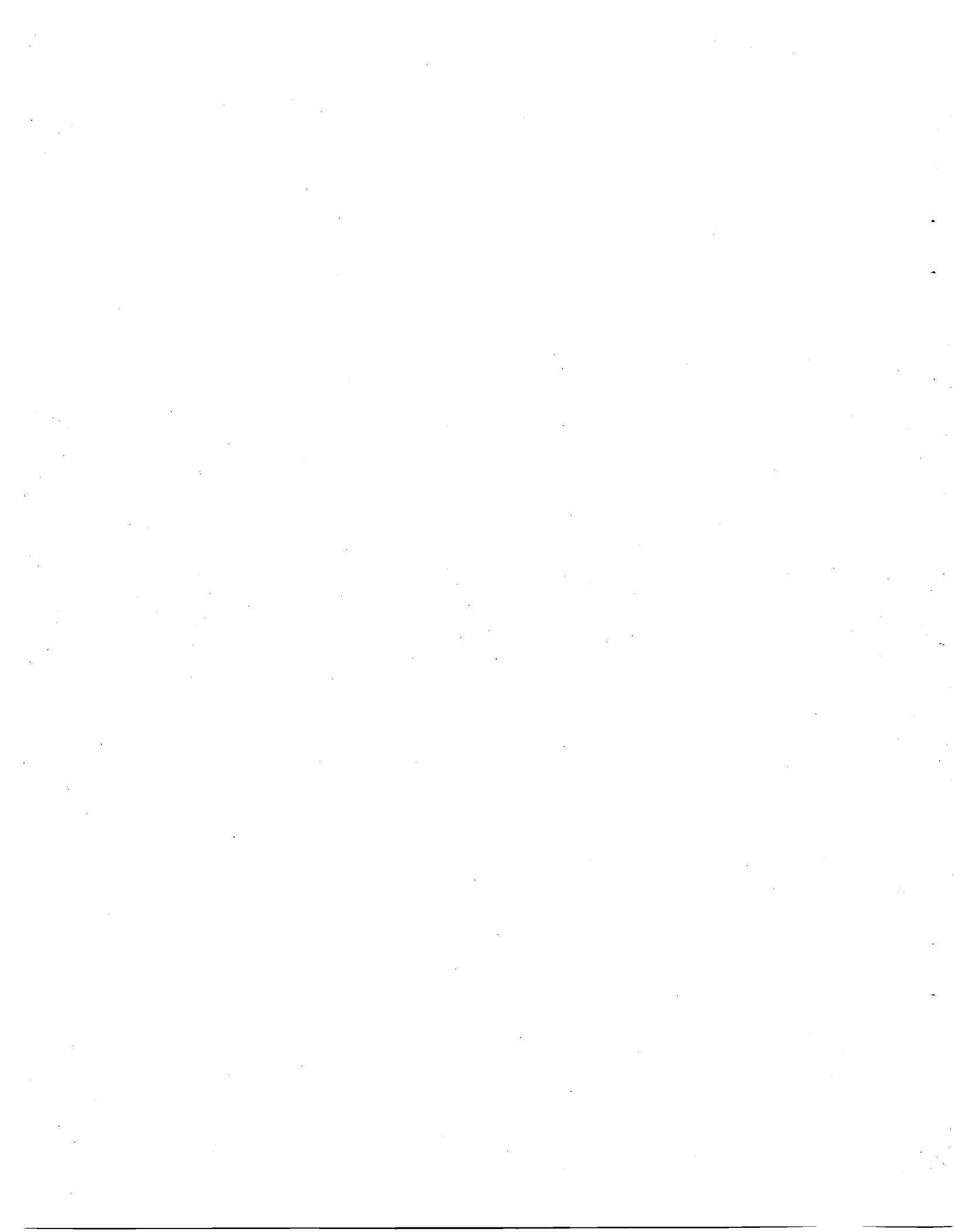


TABLE OF CONTENTS

<u>Section</u>		<u>Page</u>
	SUMMARY	1
1.0	INTRODUCTION	3
2.0	TASK 1 ATTACHMENTS	7
2.1	Task 1.1 - Design and Analysis of Attachments	7
2.1.1	Literature Survey	7
2.1.2	Design and Analysis	8
2.2	Task 1.2 - Material and Small Component Characterization	10
2.2.1	Task 1.2.1 - Design Allowables	10
2.2.2	Task 1.2.2 - Small Specimen Tests	11
2.3	Task 1.3 - Preliminary Evaluation of Attachment Concepts	24
3.0	TASK 2 BONDED JOINTS	41
3.1	Task 2.1 - Standard Bonded Joints	41
3.1.1	Task 2.1.1 - Analysis of Standard Joints	41
3.1.2	Task 2.1.3 - Ancillary Laminate and Adhesive Tests	44
3.1.3	Task 2.1.4 - Joint Specimen Fabrication and Non-Destructive Evaluation	51
3.1.4	Task 2.1.5 - Standard Joint Tests	54
3.1.5	Task 2.1.6 - Test Analysis and Correlation	54
4.0	CONCLUDING REMARKS	73
	REFERENCES	75

SUMMARY

This document reports on activities from May 1, 1980, through November 30, 1980, of an experimental program to develop several types of graphite/polyimide (GR/PI) bonded and bolted joints. The program consists of two concurrent tasks. TASK 1 is concerned with design and test of specific built-up attachments, while TASK 2 evaluates standard and advanced bonded joint concepts. The purpose is to develop a data base for the design and analysis of advanced composite joints for use at elevated temperatures [561K (550°F)]. The objectives are to identify and evaluate design concepts for specific joining applications and to identify the fundamental parameters controlling the static strength characteristics of such joints. The results from these tasks will provide the data necessary to design and build GR/PI lightly loaded flight components for advanced space transportation systems and high speed aircraft.

During this reporting period, principal program activities dealt with the literature survey, design of static discriminator specimens, design allowables testing, fabrication of test panels and specimens, small specimen testing and standard joint testing. Detail designs of static discriminator specimens for each of the four major attachment types are presented. Test results are presented for the following:

- a. Transverse (normal to laminate) tension tests of $(0/+45/90)_{2s}$ Celion 3000/PMR-15 laminate.
- b. Net tension of a $(0/+45/90)_{8s}$ laminate for both a loaded and unloaded bolt hole.
- c. Comparative testing of bonded and co-cured doublers along with pull-off tests of single and double bonded angles.
- d. Single lap shear tests [standard 12.7 mm (.5 inch) and "thick adherend"], transverse tension and coefficient of thermal expansion (CTE) tests of A7F (LARC-13 Amide-Imide Modified) adhesive.
- e. Tension tests of standard single lap, double lap and symmetric step-lap bonded joints.

Also presented are results of a finite element analysis of a single lap bonded composite joint.

SECTION 1.0

INTRODUCTION

This is the 6th quarterly report covering results of activity during the period May 1, 1980, through October 31, 1980.

The purpose of this program is to provide a data base for the design of advanced composite joints useful for service at elevated temperatures [561K (550°F)]. The current epoxy-matrix composite technology in joint and attachment design will be extended to include polyimide-matrix composites. This will provide data necessary to build graphite/polyimide (GR/PI) lightly loaded flight components for advanced space transportation systems and high speed aircraft. The objectives of this contract are twofold: First, to identify and evaluate design concepts for specific joining applications of built-up attachments which could be used at rib-skin and spar-skin interfaces; second, to explore advanced concepts for joining simple composite-composite and composite-metallic structural elements, identify the fundamental parameters controlling the static strength characteristics of such joints, and compile data for design, manufacture, and test of efficient structural joints using the GR/PI material system.

The major technical activities follow two paths concurrently. The TASK 1 effort is concerned with design and test of specific built-up attachments while the TASK 2 work evaluates standard and advanced bonded joint concepts.

The generic joint concepts to be developed under TASK 1 are shown in Figure 1-1. The total program is scheduled over a period of 27 months as shown in Figure 1-2.

In TASK 1.1, several concepts were designed and analyzed for each bonded and each bolted attachment type and reported in reference 1. Concurrent with this task a series of design allowable and small specimen tests are being conducted under TASK 1.2. The analytical results of TASK 1.1 and the design data from TASK 1.2 will allow a selection of the most promising bonded and bolted concepts.

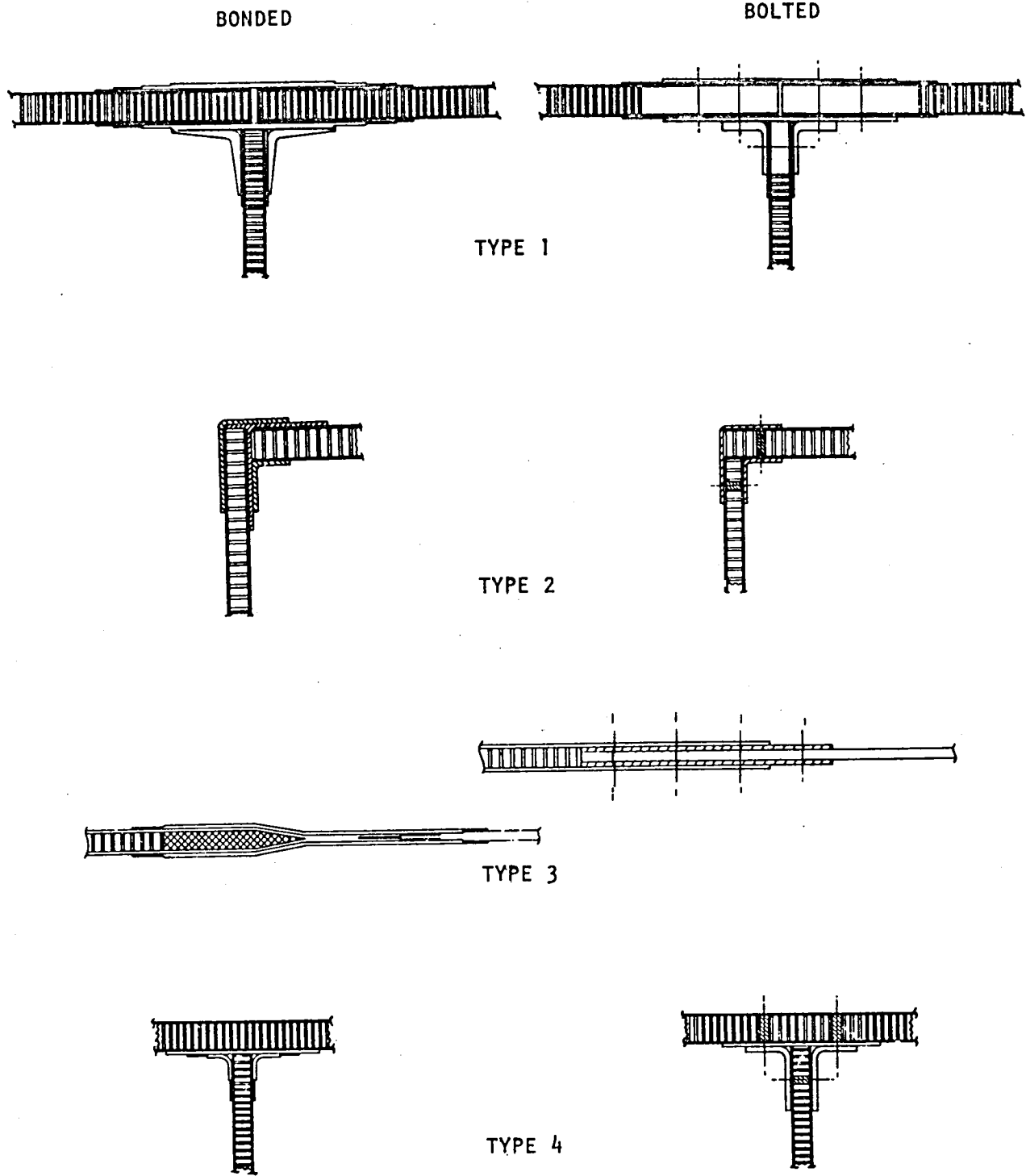


Figure 1-1: Generic Joint Concepts for 4 Attachment Types

NASA CONTRACT NAS1-15644

DESIGN, FABRICATION AND TEST OF GRAPHITE/POLYIMIDE COMPOSITE JOINTS AND ATTACHMENTS FOR ADVANCED AEROSPACE VEHICLES

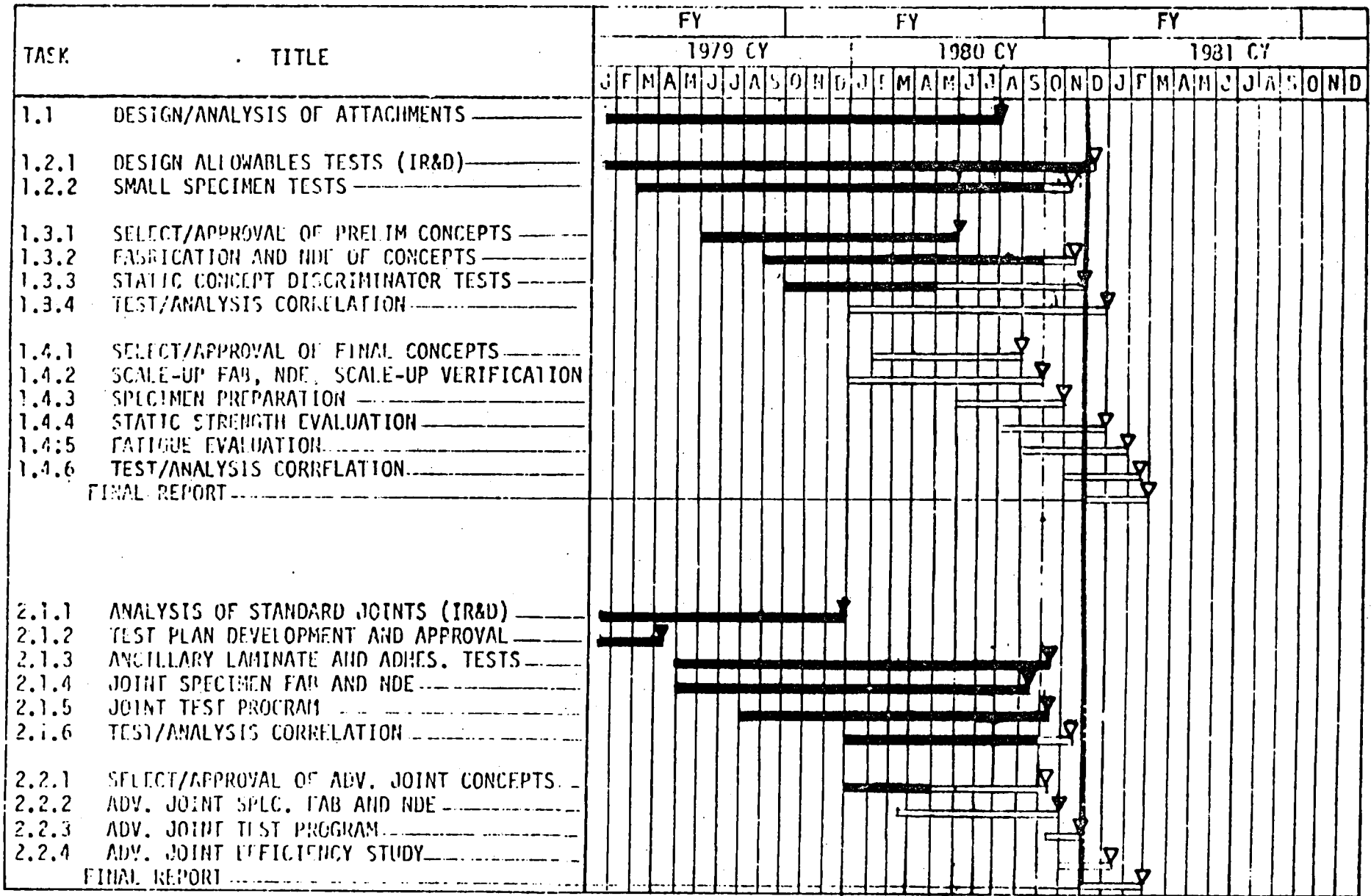


FIGURE 1-2 MASTER PROGRAM SCHEDULE

LEGEND

- ▽ ENDING DATE
- ◆ REVISED ENDING DATE

In TASK 1.3, a maximum of two of the most promising concepts for each joint type will be fabricated, tested and evaluated. The evaluation will yield the preferred joint concepts and will be based on weight efficiency, ease of fabrication, detail part count, inspectability and predicted fatigue behavior.

Finally, eight joint concepts (2 of each joint type) will be fabricated in TASK 1.4 on a scaled-up manufacturing basis to assure that reliable attachments can be fabricated for full-scale components. A series of static tests will be performed on specimens cut from the scaled-up attachments to verify the validity of the manufacturing process. Additional specimens will be thermally conditioned and tested in a series of static and fatigue tests. Test results will be compared with the analytical predictions to select final attachment concepts and design/analysis procedures.

The TASK 2 activity will establish a limited data base that will describe the influence of variations in basic design parameters on the static strength and failure modes of GR/PI bonded composite joints over a 116K to 561K (-250°F to 550°F) temperature range. The primary objectives of this research are to provide data useful for evaluation of standard bonded joint concepts and design procedures, to provide the designer with increased confidence in the use of bonded high-performance composite structures at elevated temperature, and to evaluate possible modifications to the standard joint concepts for improved efficiency.

To accomplish these objectives, activity under TASK 2.1 will consist of design, fabrication, and static tests of several classes of composite-to-composite and composite-to-metallic bonded joints including single-and-double-lap joints and step-lap joints. Test parameters will include lap length, adherend stiffness and stacking sequence at room and elevated temperatures. Toward the latter part of this program, under TASK 2.2., a selection will be made of advanced lap joint concepts which show promise of improving joint efficiency. Possible concepts are pre-formed adherends, mixed adhesive systems, and lap edge clamping. These concepts will be added to the static strength test program and the results compared with the results from the standard joint tests.

This report summarizes the literature survey, presents static discriminator test specimen designs, preliminary results of design allowables, small specimen testing, ancillary adhesive tests and standard joint tests completed during this reporting period.

SECTION 2.0

TASK 1 ATTACHMENTS

2.1 TASK 1.1 - Design and Analysis of Attachments

This section discusses the results achieved during this reporting period on the literature survey and on design and analysis of attachments.

2.1.1 Literature Survey

A comprehensive literature search was initiated at the beginning of the program to compile applicable experimental data and analyses concerned with the processing control, properties, and fabrication of GR/PI composite materials. In addition, the search was focused on design/analysis and evaluation of test data of bonded and bolted composite attachments.

The search has revealed an extensive amount of basic research, both completed and on-going, concerning attachments of composite structural members. Results of the literature search have been reported in previous Quarterly Report numbers 1, 2, 3, 4 and 5. Review of current literature is a continuous on-going process during performance of this contract. A summary of relevant literature reviewed during this reporting period is given below.

Reference 1 presents a comparison of experimentally measured stresses with those predicted by analytical, numerical and finite element solutions. Adhesive shear stresses in a plexiglass single lap joint are measured by monitoring the fringe pattern generated by a laser incident on single wires imbedded on each side of the bond layer. Results are compared to the various analytical solutions. For the particular case analyzed, it is concluded that the closed form Goland-Reissner and Plantema solutions and the numerical BOND4 program (University of Delaware) predict the best shear stress distributions. The BONJOI program (Lockheed) also gives fairly accurate predictions. Experimental boundary conditions most closely matched those of BOND4 (pinned) than those of BONJOI (clamped). The numerical solutions satisfy the condition of zero shear stress at the end of the adhesive and therefore give a better estimate of maximum shear stress.

The effect of the method of loading and specimen configuration on the measured compressive strength of graphite/epoxy (Narmco T300/5208) composite materials was investigated in Reference 2. Three test methods were conducted; an adaptation of the IITRI "wedge grip" fixture, a face supported fixture, and an end-loaded-coupon fixture. Effects of specimen size, specimen support and method of load transfer were also evaluated. Test results obtained from the three fixtures are presented and evaluated with respect to the various test parameters. It is concluded that the IITRI fixture has the best potential for unidirectional and quasi-isotropic laminates. The face supported fixture is most desirable for $[+45]_5$ laminates. Data obtained with the end-loaded-coupon fixture were not substantially different from the other test fixtures evaluated. Based on this and because of specimen simplicity, further study of the end-loaded-coupon fixture is warranted.

Reference 3 presents design guidelines and design criteria for developing bonded primary structure. It presents design information generated during the Primary Adhesively Bonded Structure (PABST) program. It discusses material selection requirements, manufacturing considerations, inspection needs, repairability and cost and weight analyses. Also presented are loads, load transfer and failure modes of bonded joints, along with analysis methods for analyzing all types of bonded joints. The final section discusses the type of testing and specimens needed to select an adhesive for use in bonded primary structure.

2.1.2 Design and Analysis

The design analysis procedure used to develop the joint designs is shown in Figure 2-1 which illustrates the interaction between design, analysis and test. Shaded areas indicate percent completion.

Basic designs for all the bonded and bolted joints are presented in the 5th quarterly Report (CR 159112). Designs presented along with the small specimen test results (Section 2.2.2) were used to arrive at the static discriminator specimen configurations discussed in Section 2.3. There was also extensive coordination with the Materials and Processes group to assure that planned

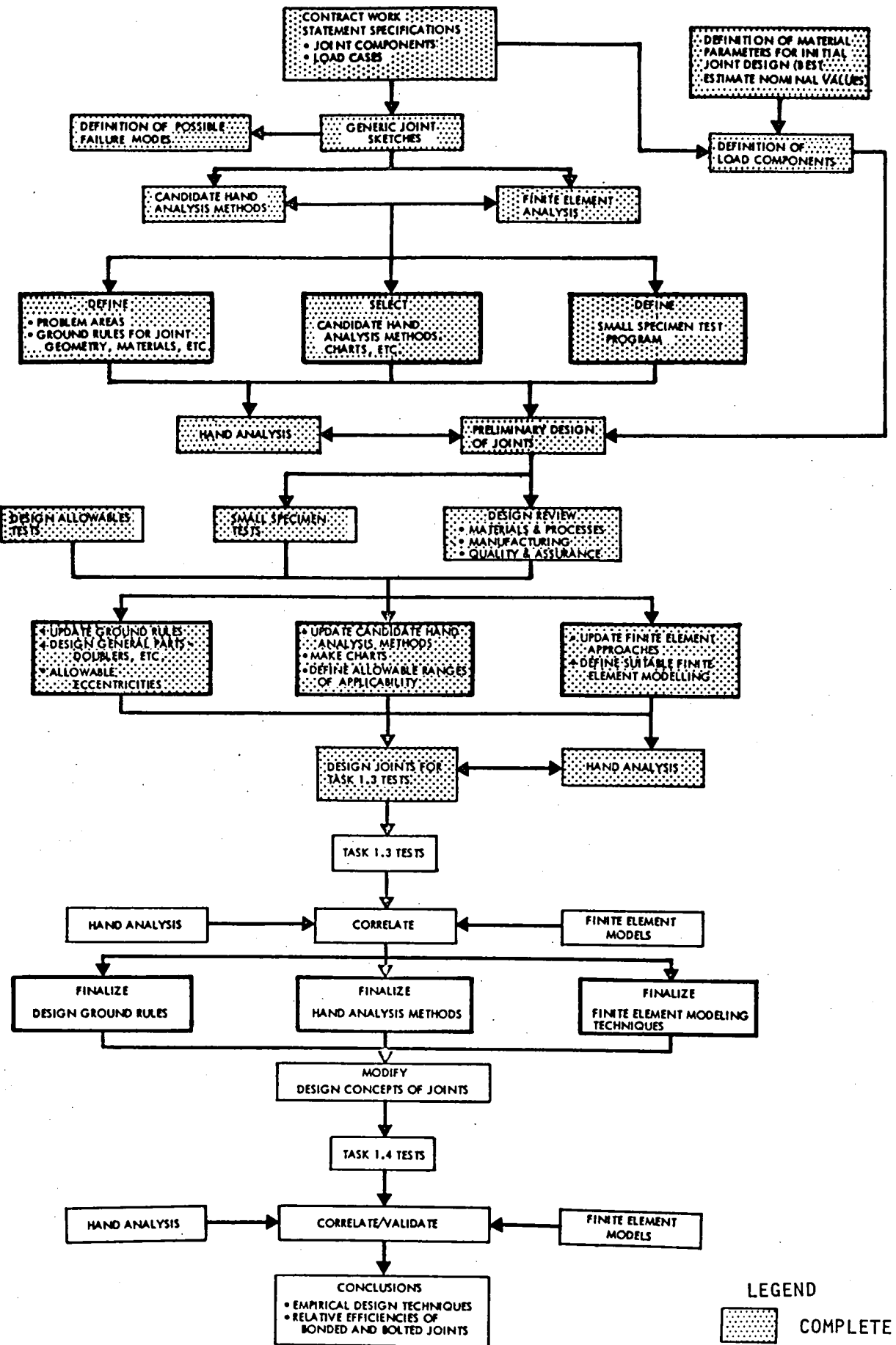


Figure 2-1: Task 1 Design/Analysis/Test Flow Diagram

processing and assembly sequencing could be achieved. This resulted in some changes to the Type 2 Bonded joint from the design presented in the 5th Quarterly Report (CR 159112). The revised Type 2 bonded joint design is as shown in Figure 2-11.

Designs for all the joint types will be finalized when the small specimens and static discriminator test are completed and results analyzed.

2.2 TASK 1.2 - Material and Small Component Characterization

This section discusses design allowables and small specimen testing.

2.2.1 TASK 1.2.1 - Design Allowables

Results of limited design allowables testing conducted on Celion 3000/PMR-15 laminates under this contract are presented in the 5th Quarterly Report (CR 159112). Results of other design allowables testing conducted during this reporting period are discussed below.

Flatwise laminate-to-laminate tension tests have been completed for a Celion 3000/PMR-15 (0,+45,90)_{2s} laminate. Tests were conducted on cured/post-cured specimens and on specimens aged 125 hours at 589K (600°F). Specimen configuration and test results are shown in Figure 2-2. The reduction in transverse strength at elevated temperature is as expected since this is a matrix dominated property.

Coefficient of thermal expansion (CTE) tests were conducted on cured/post-cured A7F (LARC 13 amide-imide modified) adhesive. Test results are given in Table 2-1.

Table 2-1: CTE Data A7F Adhesive

Material	Condition	Mean Temp. °K	CTE mm/mm - °K
A7F	Cured/Post-Cured	279	2.657x10 ⁻⁵
		385	3.031x10 ⁻⁵
		483	3.541x10 ⁻⁵

2.2.2 TASK 1.2.2 - Small Specimen Tests

Comparative testing of bonded versus co-cured doublers was conducted to evaluate the load transfer efficiency for application to bolted joints. Tests were conducted on "cured/post-cured" and "aged 125 hrs at 589°K (600°F)" specimens. Specimen configuration and test set-up are shown in Figures 2-3 and 2-4, respectively. A comparison of test results is shown in Table 2-2. The failure modes were the same in all specimens, with the exception that some failed in the tab area. Bonded doublers failed at lower loads than the co-cured doubler. It is concluded that the co-cured doubler is stronger and will be used for Task 1.3 static discriminator specimens.

Net-tension stresses at failure of a $(0, \pm 45, 90)_{8S}$ graphite polyimide laminate for both unloaded and loaded bolt holes are shown in Figures 2-5 and 2-6, respectively. The slight increase in failure stress at elevated temperature for an unloaded bolt hole (see Figure 2-5) is caused by a softening of the matrix material. This makes the laminate behave more plastically with a corresponding reduction in severity of stress concentration at the hole edge. The corresponding effect is masked for the loaded hole test because the failure mode changes from net-tension to bearing (except for two of the Condition 2 specimens, see Figure 2-6).

Small specimen tests were also conducted to evaluate the tensile strength of bonded angles. Both single and double angle specimens, as shown in Figures 2-7 and 2-8 were tested. Test results are summarized in Tables 2-3 and 2-4. Because of the very low failure loads at room temperature for the single angle, it was decided not to run the elevated temperature tests. In addition, the specimen bond lines were of very poor quality. Since the double angle met the design load requirement of 28.7 KN/m (164 lbs/in) it was decided not to rerun the single angle test. Static discriminator specimens must have the equivalent of a double angle bond to meet the design requirements.

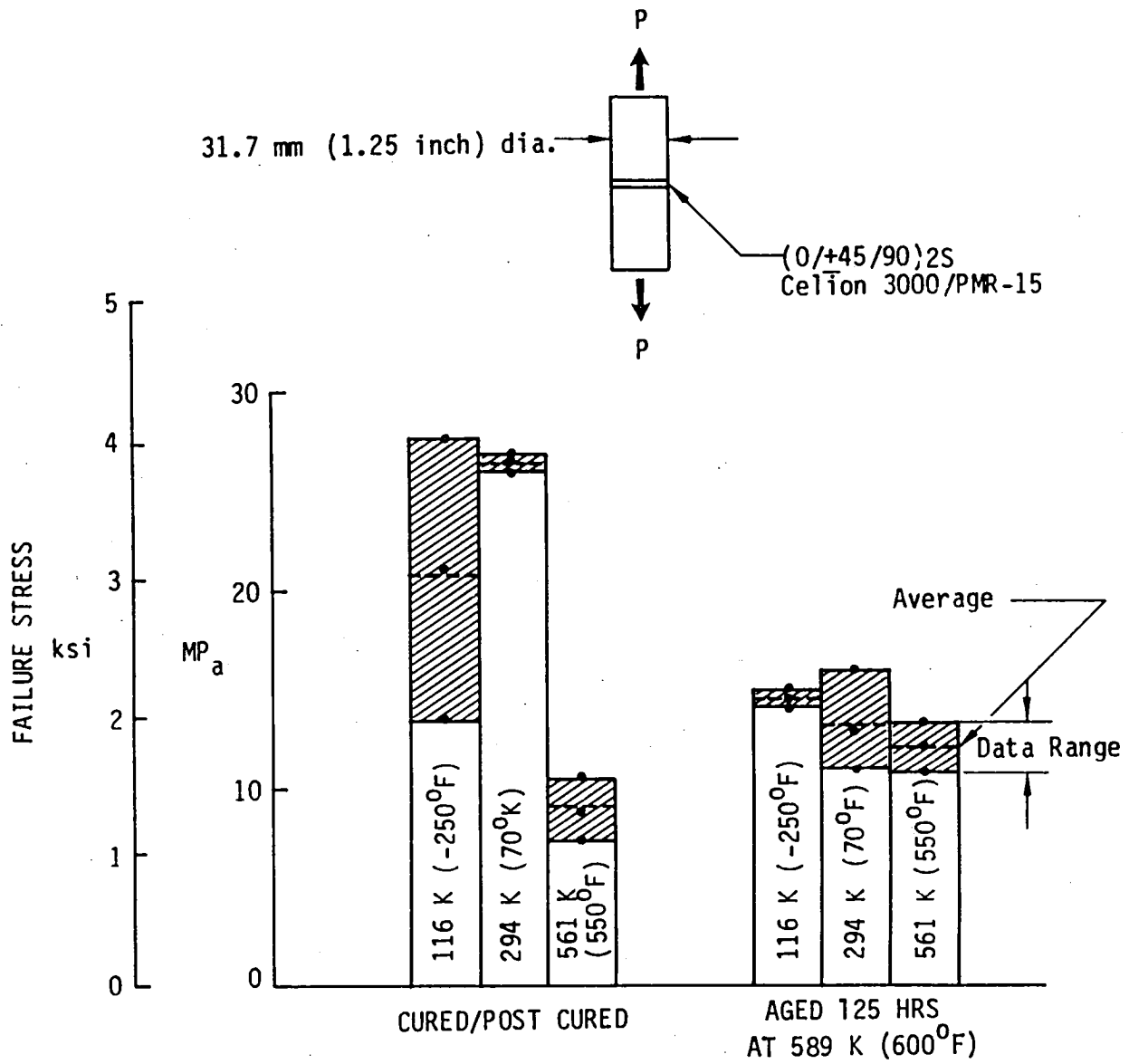
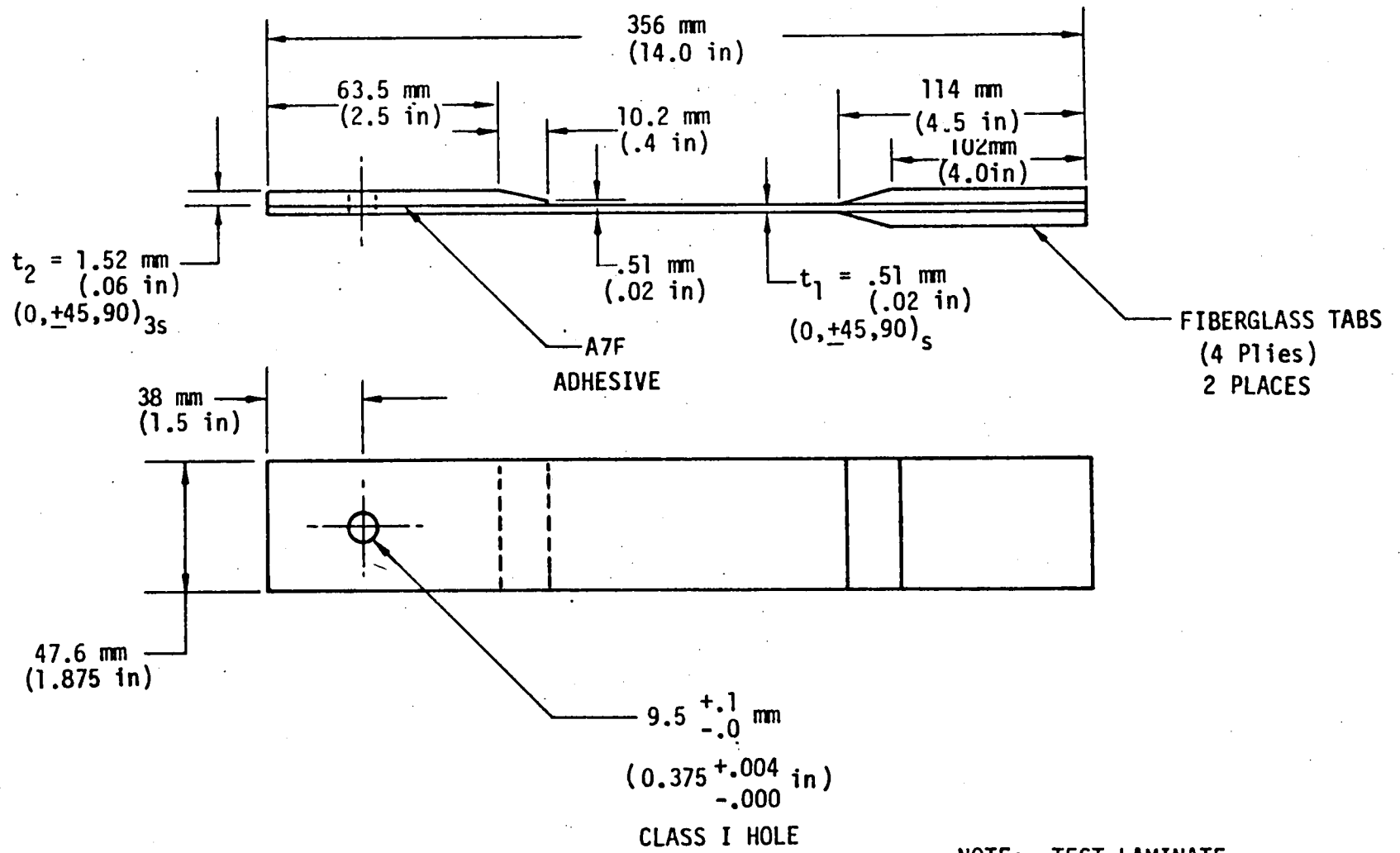


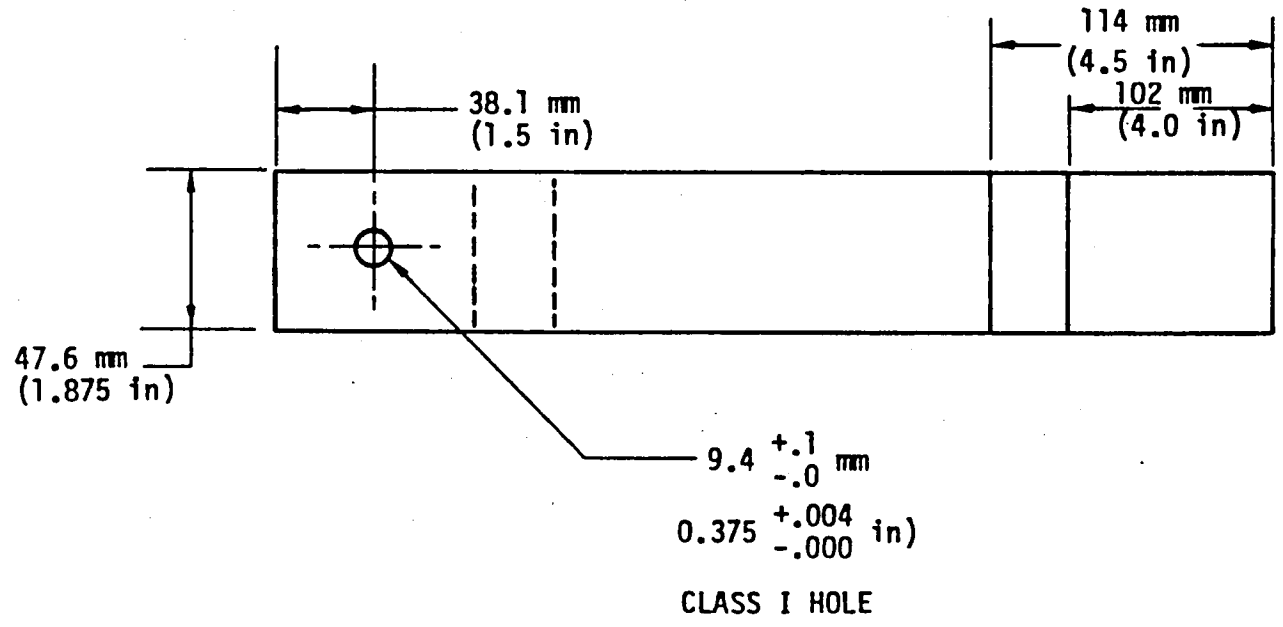
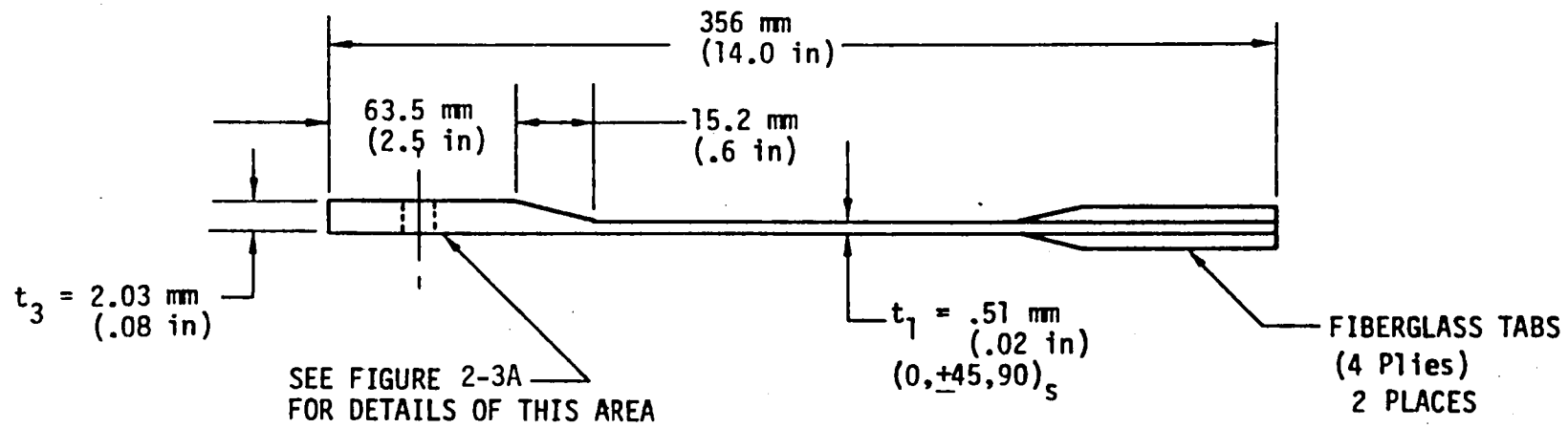
Figure 2-2 Flatwise Laminate Tension Matrix 1 Test 7



NOTE: TEST LAMINATE
CELION 3000

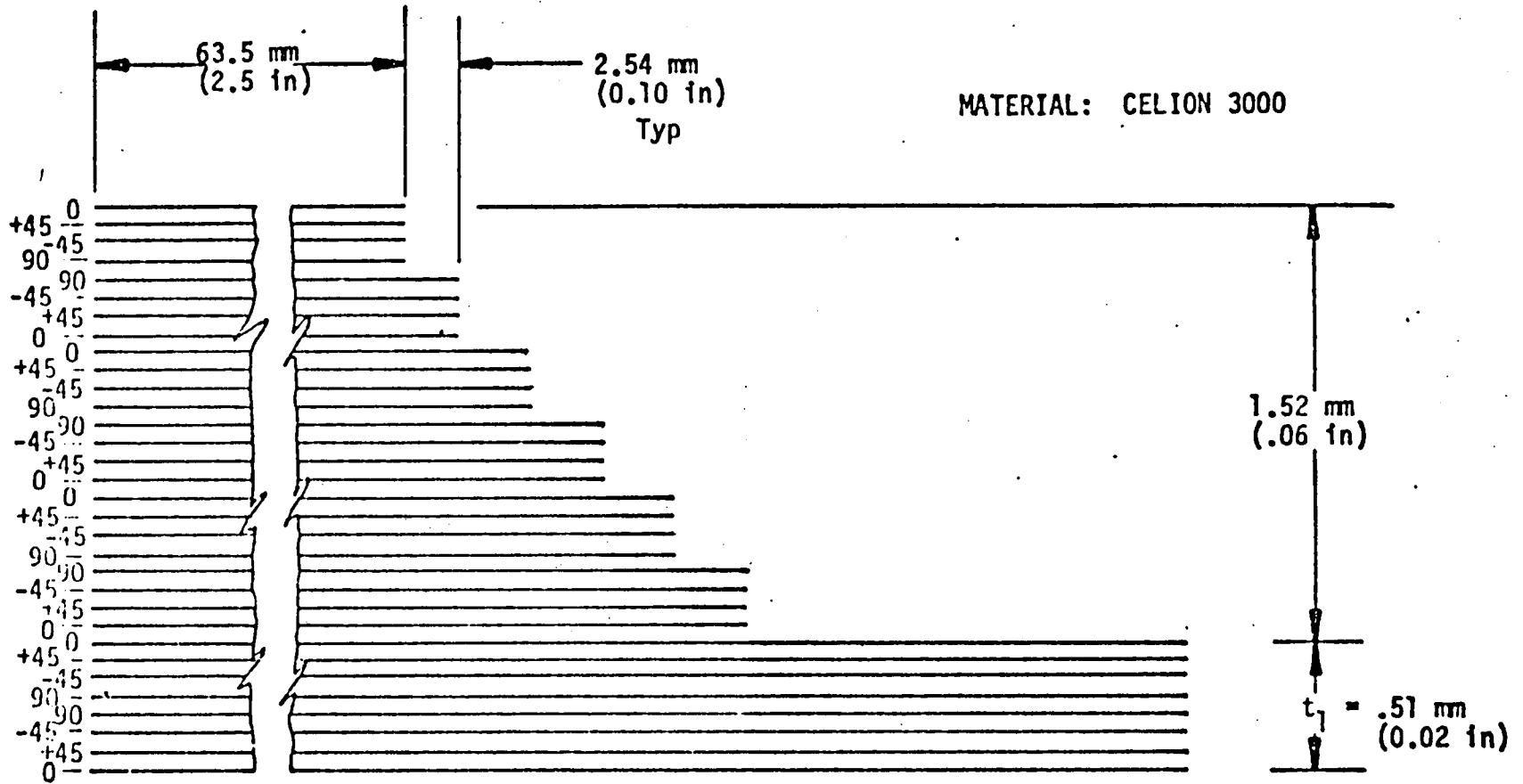
SPEC 4B-1 BONDED DOUBLER

Figure 2-3 SMALL SPECIMEN TESTS



SPEC 4B-2 INTEGRAL DOUBLER

Figure 2-3 SMALL SPECIMEN TESTS (Cont.)



SPEC. 4B-2

Figure 2-3A SMALL SPECIMEN TESTS

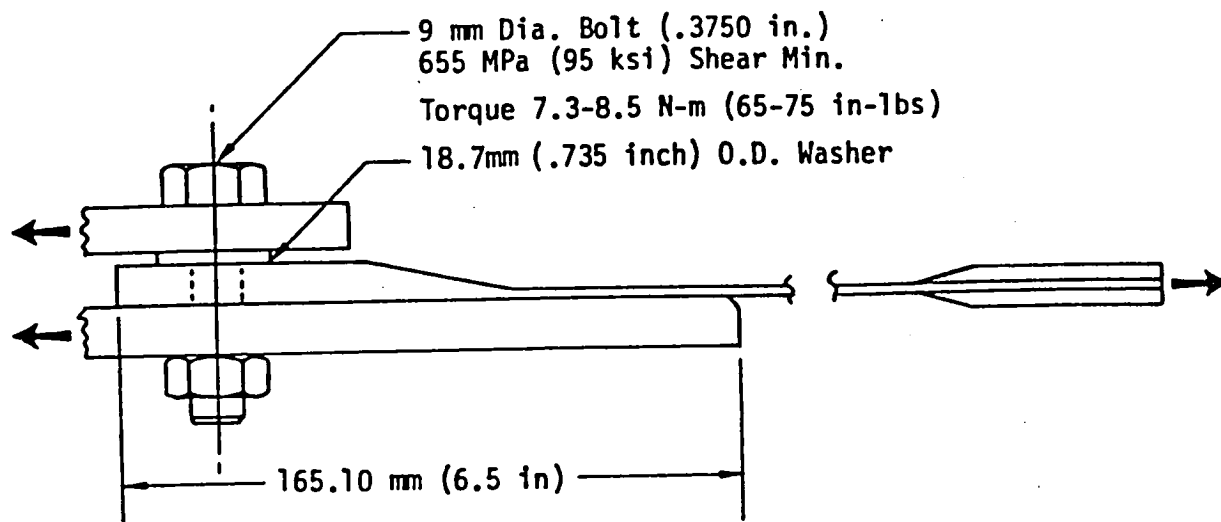


Figure 2-4 Test Setup, Matrix 4B, Tests 1a, 1b, 1c, 2a, 2b, 2c

TABLE 2-2 : Comparison of Integral and Bonded Doublers
 Matrix 4B Small Specimens
 (English Units)

COND. CODE	TEST TEMP. °F	ULTIMATE FAILURE							
		INTEGRAL DOUBLER				BONDED DOUBLER			
		LOAD kip	BRG. STRESS ksi	NET TENSION STRESS DBLR/LAM. ksi	LAMINATE STRESS ksi	LOAD kip	BRG. STRESS ksi	NET TENSION STRESS DBLR/LAM. ksi	LAMINATE STRESS ksi
1	70	2.58	80.9	20.1/76.7	61.4	1.64	46.4	11.6/46.3	37.0
		2.97	91.3	22.7/90	72.0	2.13	59.7	14.9/63.4	50.7
		2.73	85.3	21.2/84.5	67.7	2.31	65.1	16.3/67.5	54.0
	550	2.36	73.4	18.2/73.1	58.5	2.23	62.7	15.7/63.8	51.0
		2.16	67.2	16.7/66.6	53.5	2.06	57.2	14.3/57.5	46.0
		2.24	69.3	17.2/64.3	51.9	2.17	61.4	15.3/60.3	48.2
2	70	2.28	69.7	17.3/71.0	56.8	2.25	64.2	16.1/65.2	52.2
		2.08	65.1	16.2/65.1	52.1	1.94	53.4	13.4/57.0	45.6
		2.66	84.1	20.9/84.5	67.6	1.96	57.3	14.3/55.6	44.5
	550	2.31	70.3	17.5/72.3	57.8	1.82	50.0	12.5/53.7	43.0
		2.27	72.4	18.0/67.5	54.0	1.84	51.0	12.8/51.8	41.4
		2.32	73.5	18.3/72.3	57.6	1.80	50.0	12.5/50.8	40.6

Condition Code

- 1 Cured/Post Cured
- 2 Aged 125 hrs at 589K (600°F)

TABLE 2-2 : Continued - Comparison of Integral and Bonded Doublers
Matrix 4B Small Specimens

(Metric Units)

COND. CODE	TEST TEMP K	ULTIMATE FAILURE							
		INTEGRAL DOUBLER				BONDED DOUBLER			
		LOAD Kn	BRG. STRESS Mpa	NET TENSION STRESS DBLR/LAM. Mpa	LAMINATE STRESS Mpa	LOAD Kn	BRG. STRESS Mpa	NET TENSION STRESS DBLR/LAM. Mpa	LAMINATE STRESS Mpa
1	294	11.5	558	139/529	423	7.3	320	80/319	255
		13.2	629	157/620	496	9.5	412	103/437	350
		12.1	588	146/583	467	10.3	449	112/465	372
	561	10.5	506	125/504	403	9.9	432	108/440	352
		9.6	463	115/459	367	9.2	394	96/396	317
		10.0	478	119/443	358	9.7	423	105/416	332
2	294	10.1	481	119/490	392	10.0	443	111/450	360
		9.3	449	112/449	359	8.6	368	92/399	314
		11.8	580	144/583	466	8.7	395	99/383	307
	561	10.3	485	121/498	399	8.1	345	86/370	296
		10.1	499	124/465	372	8.2	352	88/357	285
		10.3	507	126/498	399	8.0	345	86/350	280

Condition Code

- 1 Cured/Post Cured
- 2 Aged 125 hrs at 589K (600°F)

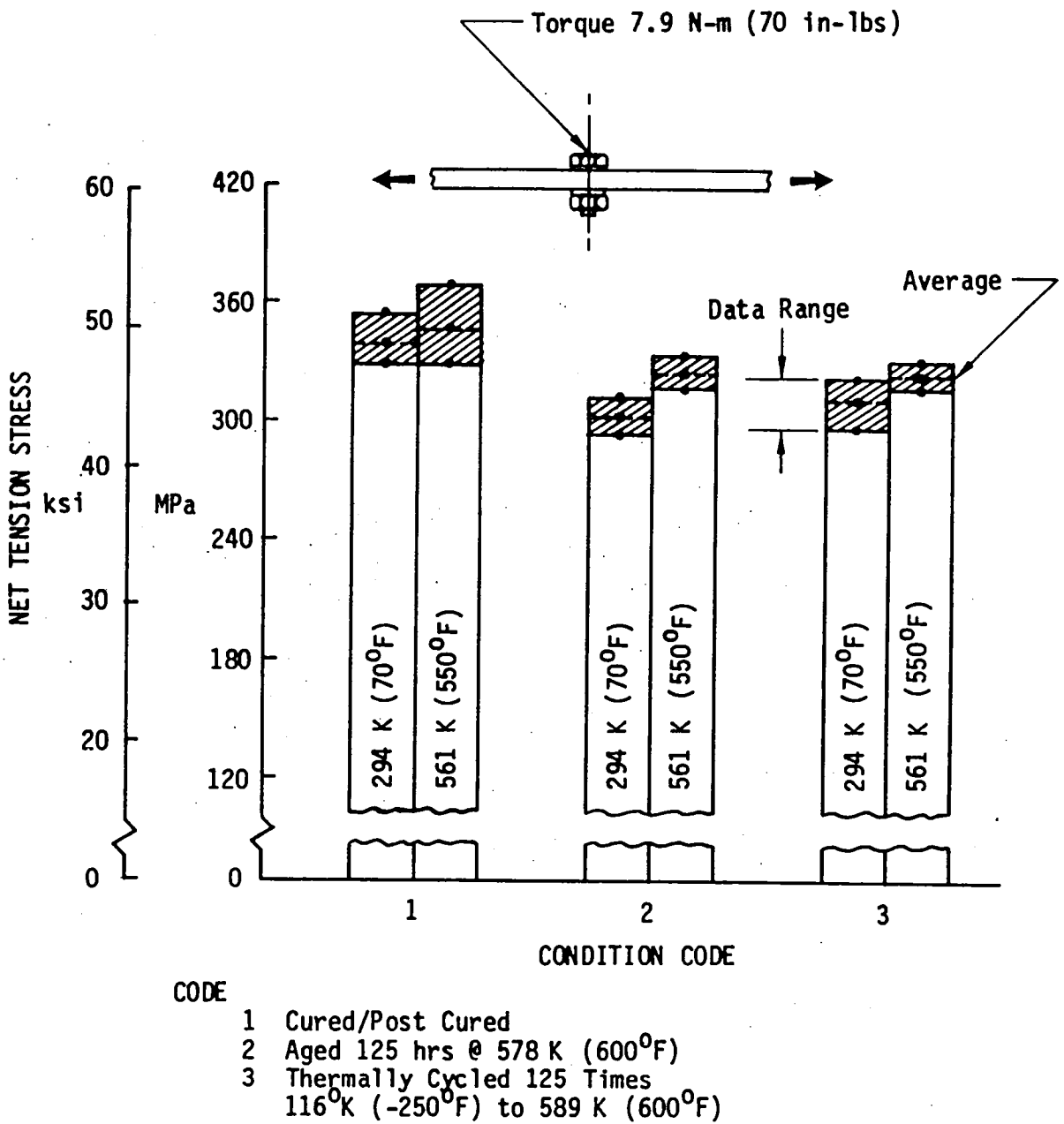
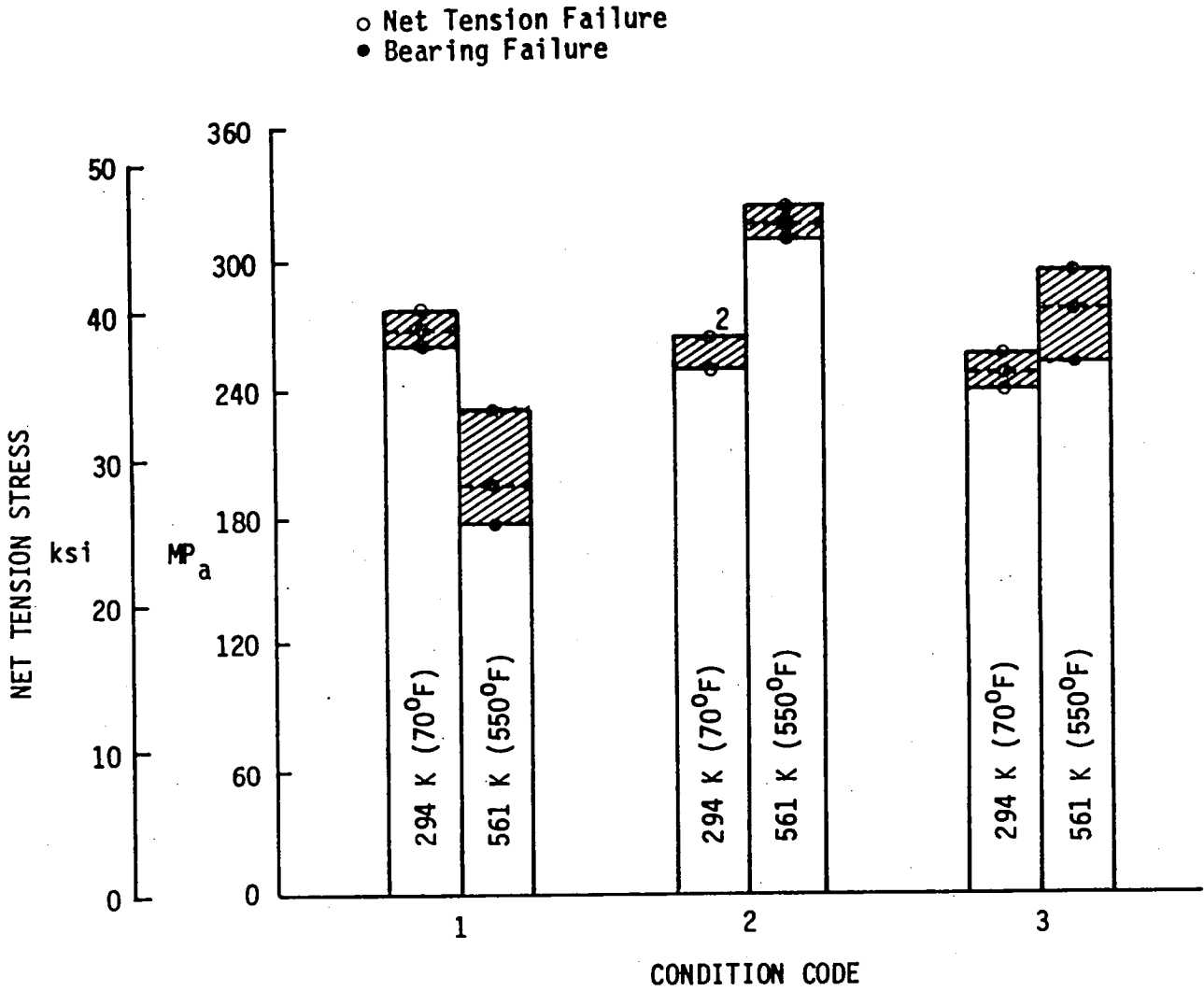


Figure 2-5 Celion 3000/PMR-15 (0, +45, 90)_{8S}, Net Tension Tests
Unloaded But Filled Hole 95 mm (3/8") Bolt W/D = 5

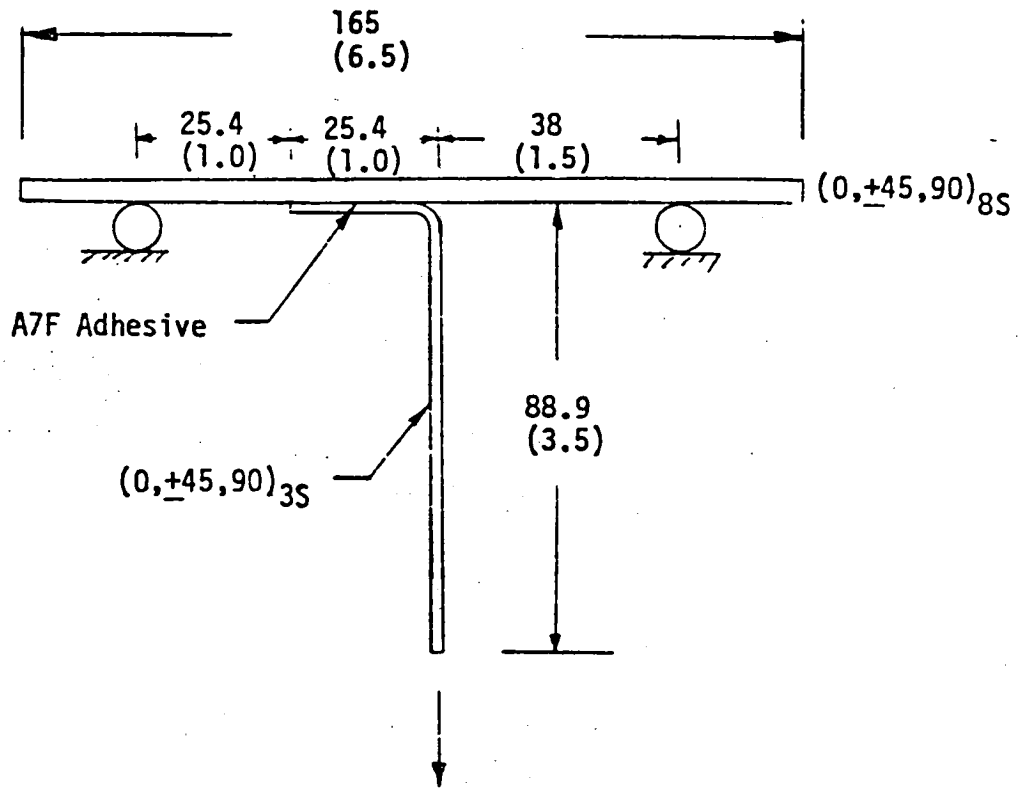


CODE

- 1 Cured/Post Cured
- 2 Aged 125 hrs @ 589 K (600°F)
- 3 Thermally Cycled 125 Times
116^oK (-250^oF) to 589 K (600^oF)

Figure 2-6 Celion 3000/PMR-15, (0, +45, 90)_{8S}, W/D = 3.5, e/D = 3.5
 Net Tension—Loaded Bolt 95 mm (3.8") Bolt
 Torqued 7.3-8.5 N-m (65-75 in-lbs)

Figure 2-7 MATRIX 4C Test 1a Revised
Cured/Post Cured

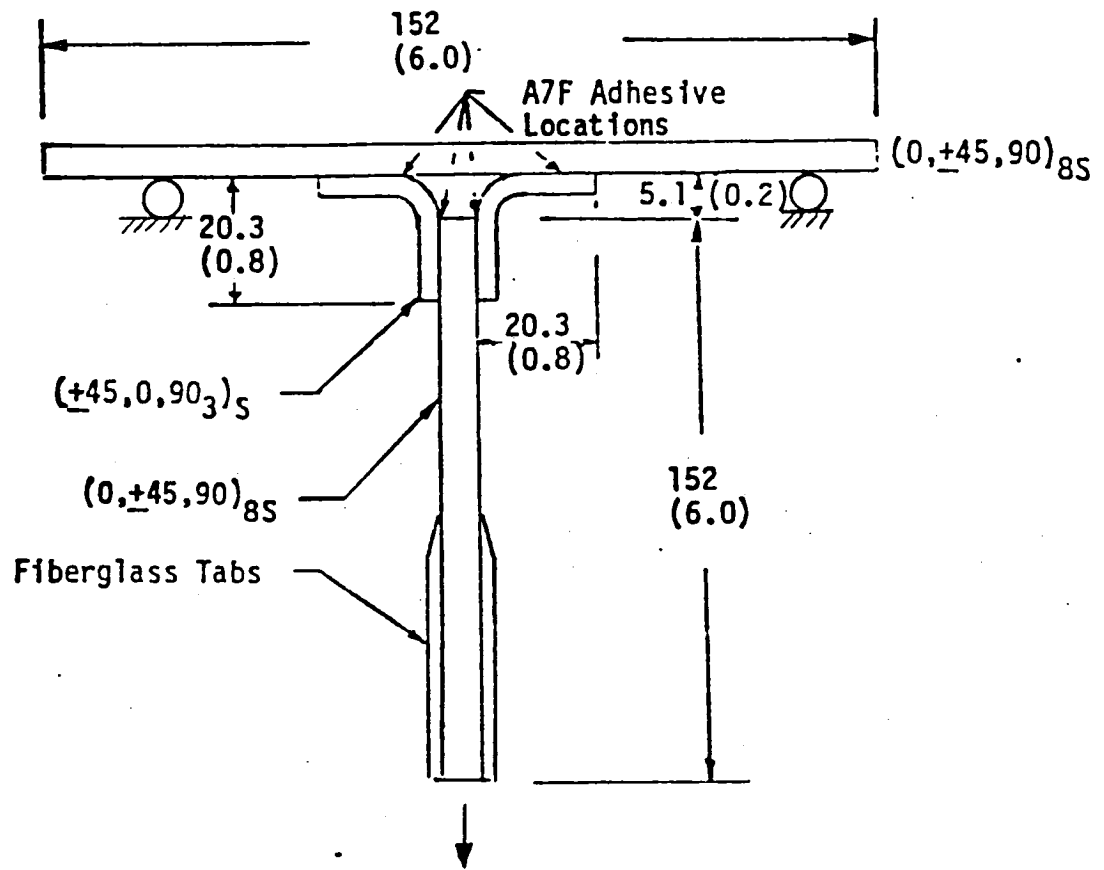


Spec. 25.4 (1.0) Wide

Dimensions $\frac{\text{mm}}{\text{(inch)}}$

Figure 2-8

MATRIX 4C Test 2b Revised
Aged 125 hrs @ 589K (600°F)



Spec. 25.4 (1.0) Wide
6 Req'd.

Dimensions mm
 (inch)

Table 2-3 Matrix 4C Test 1a Results
Single Angle Pull-Off

Spec. No.	Condition	Temperature K (°F) 	Failure Load N (1b)
4C-1a-1-1	Cure/Post-cured	294 (70)	248 (55.8)
4C-1a-1-3	"	294 (70)	232 (52.1)
4C-1a-1-4	"	294 (70)	292 (65.6)

Note: See Figure 2 for Spec. Configuration

 Elevated Temperature Tests were not run because of low failure loads at room temperature.

Table 2-4 Matrix 4C Test 2b Results
Double Angle Pull-Off

Spec. No.	Condition	Temperature °K(°F)	Failure Load N (1b)
4C-2b-2-1	Aged*	294 (70)	1032 (232)
4C-2b-2-2	"	294 (70)	765 (172)
4C-2b-2-3	"	294 (70)	1263 (284)
4C-2b-2-4	"	561 (550)	1366 (307)
4C-2b-2-5	"	561 (550)	1076 (242)
4C-2b-2-6	"	561 (550)	1134 (255)

* Aged 125 Hrs at 589°K (600°F)

2.3 TASK 1.3 - Preliminary Evaluation of Attachment Concepts

Designs for all the static discriminator specimens, except Type 3 bonded, have been finalized and fabrication started. Detailed drawings are shown in Figures 2-9 through 2-15. Detail design of Type 3 Bonded joints will be finalized upon completion of testing and data analysis of the symmetric step-lap standard joints of Matrix 3G (see Section 3.1.5).

Specimen fabrication has been started by initially laying up the required skin panels. Required fasteners and high temperature potting material, BMS 8-126, has been received. Specimens are being fabricated from material lots 2W4781 and 2W4809. Mechanical Q.C. data for these lots are given in Table 2-5.

Type 1 bonded (SK 2-078001) and Type 1 bolted (SK 2-078002) static discriminator test specimens will be loaded by tension only in the plane of the cover. To reduce specimen costs, the web and web attach angles have been deleted since they do not contribute to the primary load path. The stiffness of the bonded on "T" for the Type 1 bonded joint has been simulated by bonding on an equivalent thickness "doubler" of GR/PI to the lower splice plate.

Laminates for the skins on the Type 4 bonded and bolted joints are unsymmetric lay-ups. This was done to try and get the thinnest possible laminate while still maintaining symmetry about the sandwich midplane as requested in the statement-of-work. The unsymmetric laminates cannot be precured and bonded to the core; therefore, they will be co-cured on the core. Precured laminates are cured at 1.38 MPa (200 psi), however, to prevent core crushing, the co-cured panels will be limited to 0.69 MPa (100 psi) maximum. The lower cure pressure will result in lower strength allowables for the co-cured laminates, however, they will still have adequate strength for the Type 4 joint. These specimens will give valuable experience and design data to assess the desirability of co-curing very thin, high temperature laminates.

Adhesive film for "Small Specimens" and "Standard Joints" testing to date has been made by hand troweling the adhesive resin onto fiberglass scrim cloth. Hand troweling is impractical for the larger bond areas required in the static strength test specimens. Premixed adhesive resin (LARC-13 Amide-Imide













Table 2-5: Quality Control Data

PROPERTY		REQUIREMENT	LOT NUMBER	
			2W4781 (20 lbs)	2W4809 (10 lbs)
Fiber Volume, %		58 \pm 2	N.A.	N.A.
Resin Content, %		30 \pm 3	41.5	3.8
Specific Gravity g/cc		1.54	N.A.	N.A.
Void Content, %		1	N.A.	N.A.
Flexural Strength MPa (ksi)	At Ambient	1515 (220)	1489 (216)	1351 (196)
	At 589K (600°F)	757 (110)	636 92.2	698 (101.2)
	Aged, at 589K (600°F)	757 (110)	N.A.	1040 (150.8)
Flexural Modulus GPa (msi)	At Ambient	117 (17)	135 (19.6)	139 (20.1)
	At 589K (600°F)	103 (15)	110 (16)	110 (16.0)
	Aged, at 589K (600°F)	103 (15)	N.A.	107 (15.5)
Short Beam Shear Strength MPa (ksi)	At Ambient	96 (14)	93 (13.5)	93 (13.5)
	At 589K (600°F)	41 (6)	47.5 (6.9)	62.7 (9.1)
	Aged, at 589K (600°F)	41 (6)	N.A.	64.9 (6.8)

Modified) has been supplied to a vendor for commercial application to the fiberglass scrim cloth. This will assure better uniformity in the adhesive film thickness and easily provide the larger quantities needed. Enough adhesive film has been ordered to complete the contract.

The static discriminator test plan (Reference Boeing Letter 2-3614-DP70-354 dated 23 May 1980) has been approved by the NASA COR, Dr. P. A. Cooper.

SECTION 3.0

TASK 2 - BONDED JOINTS

3.1 TASK 2.1 - Standard Bonded Joints

This task includes the analysis, fabrication and static strength determination of several standard bonded joint configurations. The theoretical influence of geometric and material parameters are being investigated and a test/analysis correlation performed to determine the relative efficiencies of the various joint configurations. The relationships of the sub-task activities are shown in Figure 3-1.

This section discusses analysis of standard joints, ancillary laminate and adhesive tests, joint specimen fabrication and NDE, and joint test program.

3.1.1 TASK 2.1.1 - Analysis of Standard Joints

L. J. Hart-Smith suggests three distinct failure modes in a single lap bonded composite joint: 1) failure of the adherend outside the bonded region because of additional bending stresses, 2) failure of the adhesive in shear, and 3) failure of the composite at the interface near the end of the joint because of "peel" stresses in the adhesive or laminae.

Examination of the failed single lap joints tested for this program suggests the 3rd type of failure governed in nearly all cases. Therefore, any change that can reduce the peel stress, σ_y , in the adhesive and in the lamina adjacent to the adhesive should increase the efficiency of the single lap joint.

An elastic, geometrically nonlinear finite element analysis was performed on a graphite/polyimide to graphite/polyimide single lap bonded joint. The joint was loaded in tension in three steps; $P_1 = 4318 \text{ N/cm}$ (25 lb/in), $P_2 = 87.5 \text{ N/cm}$ (50 lb/in), $P_3 = 175 \text{ N/cm}$ (100 lb/in). Based on symmetry, one-half the joint was modeled. Joint model, boundary conditions and material data used are shown in Figure 3-2.

The finite element analyses considered two layups for comparison: the 1st $(0_3/+45_3/90_3)_S$ (model #4) and the 2nd $(+45_3/0_3/90_3)_S$ (model #5). The

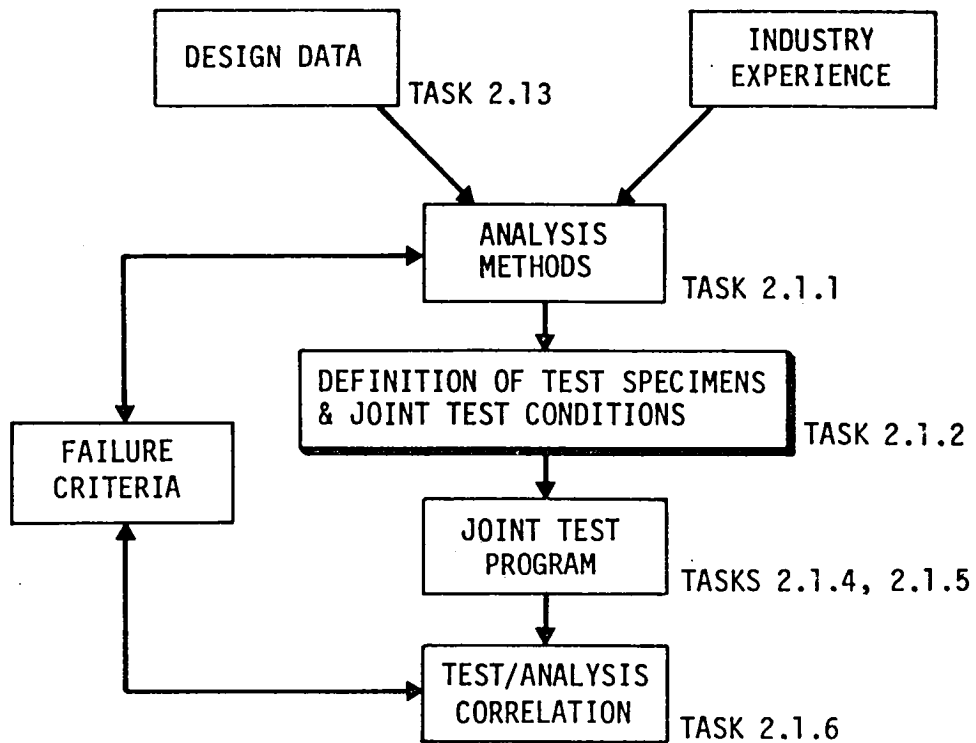
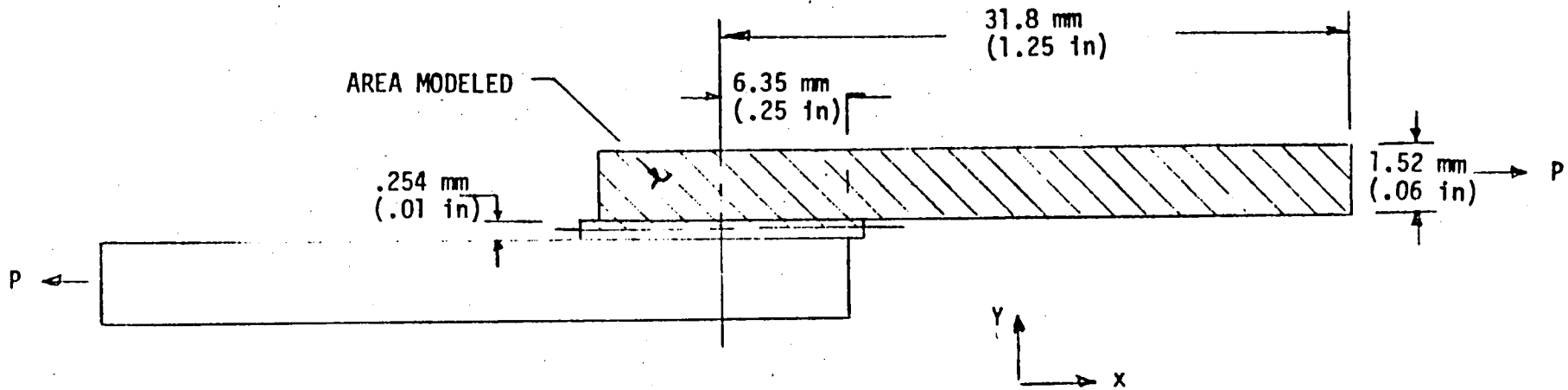
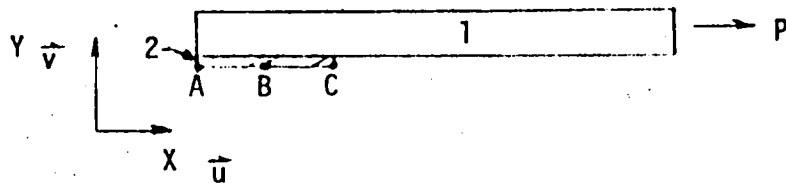


Figure 3-1: Task 2 Bonded Joint Subtasks



43



MATERIAL DATA

1 GR/PI	$E_1 = 137 \text{ GPa}$ ($20 \times 10^6 \text{ psi}$)
	$E_2 = 11 \text{ GPa}$ ($1.6 \times 10^6 \text{ psi}$)
	$\nu = .25$
	$G_{12} = 5.8 \text{ GPa}$ ($.85 \times 10^6 \text{ psi}$)

2 ADHESIVE $G = 2.1 \text{ GPa}$ ($.309 \times 10^6 \text{ psi}$)
(Assumed Homogeneous & Isotropic)

BOUNDARY CONDITIONS

A & C $\bar{u}_A = -\bar{u}_C$

B $\bar{u} = \bar{v} = 0$

Figure 3-2 GRAPHITE POLYIMIDE BONDED SINGLE-LAP JOINT

extensional stiffness of the two layups is the same, but the bending stiffness of the 1st is considerably greater than the 2nd.

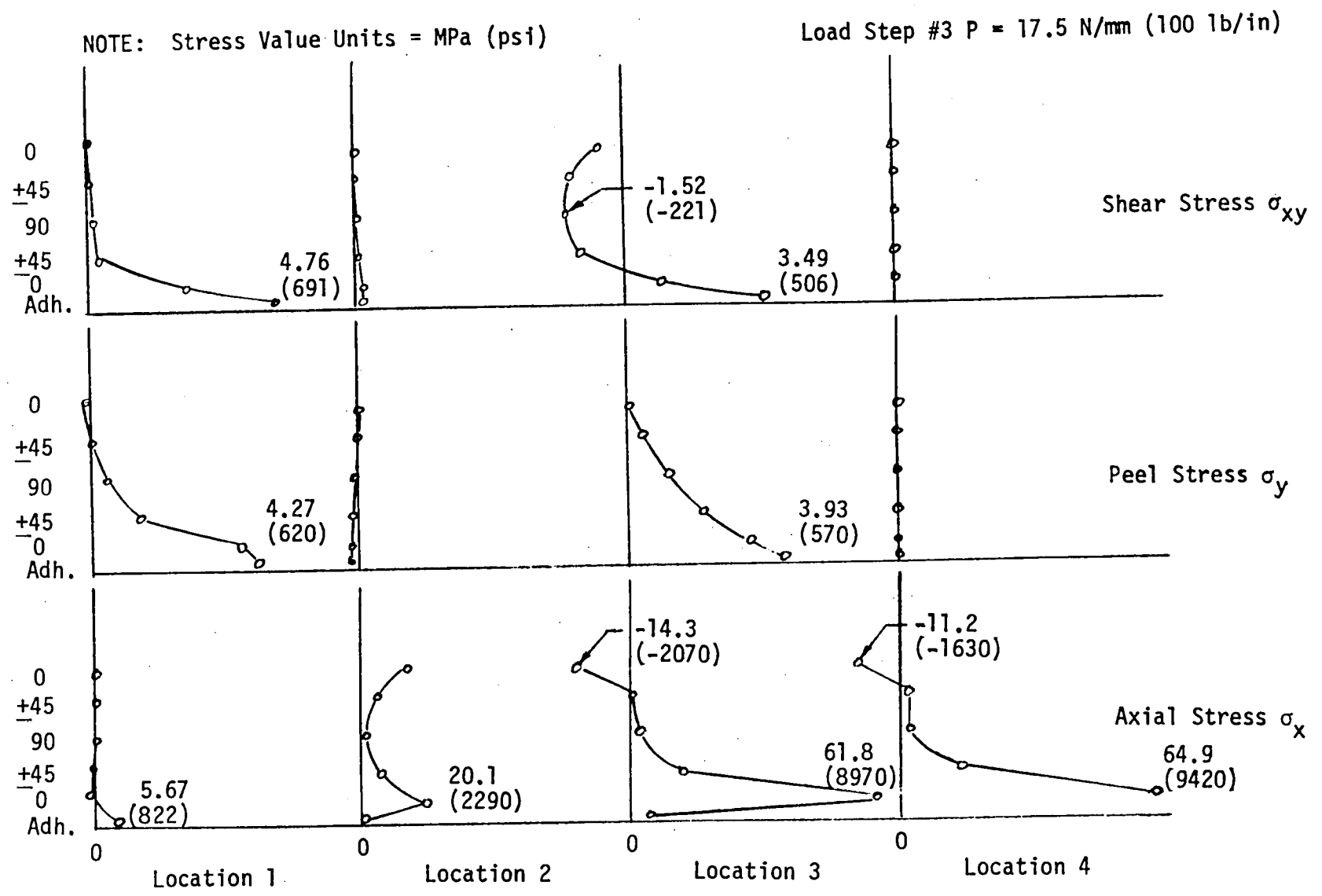
Stress distributions through the thickness of the joint are shown in Figures 3-3 and 3-4 for the two models. A comparison between them shows greater peel stresses in the adhesive for the 2nd layup (model 5). Peak peel stresses near the edge of the joint are approximately 30% greater. Shear stresses in the adhesive do not change significantly. Analysis results indicate that if the peel stresses are governing the joint failure, it is advantageous to increase the adherend bending stiffness.

3.1.2 TASK 2.1.3 - Ancillary Laminate and Adhesive Tests

Standard 12.7 mm (0.5 in) single lap titanium-to-titanium shear tests of A7F adhesive (Matrix 2, Test 3) have been completed. The titanium adherends were 1.04 mm (.041 in) thick. Test results are shown in Figure 3-6 indicating that all specimens exceeded the minimum requirement of 10.3 MPa (1500 psi). The data indicate a significant drop in shear strength due to aging and thermal cycling. Cured/post-cured specimens showed a significant drop in shear strength at elevated temperature. The aged specimens, however, exhibited essentially the same shear strength over the entire temperature range. The aging did not appear to cause excessive oxidation at the free edges of the specimens. The thermally cycled specimens failed adhesively with a characteristic silver/gray color on the adherends. This indicates a possible deterioration of the aluminum powder in the adhesive formulation or its interaction with other constituents.

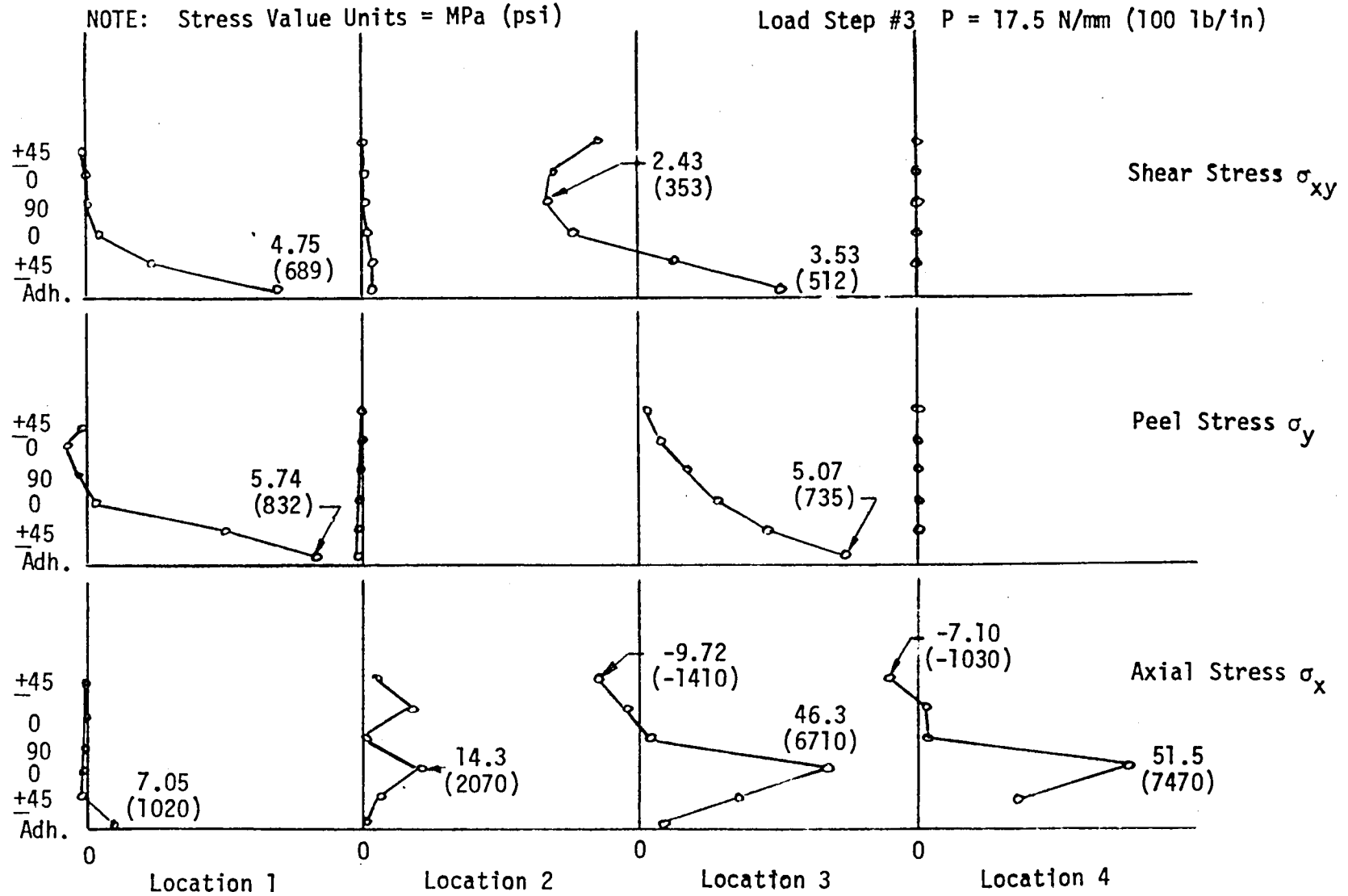
A preliminary copy of the final report for the thick adherend A7F adhesive tests conducted by Dr. J. R. Vinson at the University of Delaware has been received. A summary of the test results is given in Table 3-1 through 3-6. Since the thick adherend tests reduce peel stresses, it was expected that ultimate shear strengths would be higher than shown. Also, shear modulus and strain to failure data indicate an adhesive significantly more ductile than had been anticipated.

Tension tests of A7F adhesive bonding 31.8 mm (1.25 in) diameter stainless steel bars end-to-end (Matrix 2, Test 5) have been completed for the cured/



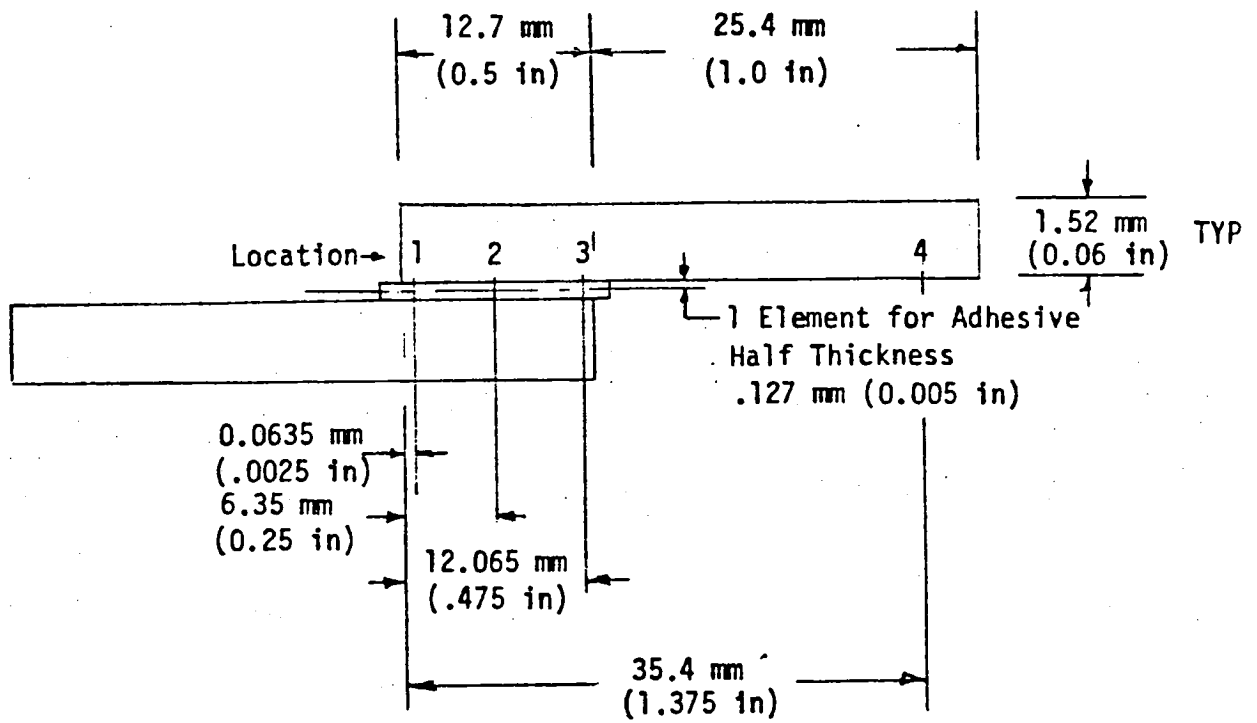
See Figure 3-5 For Location of Stress Plots

Figure 3-3 STRESS THROUGH THICKNESS Model #4



See Figure 3-5 for Location of Stress Plots

Figure 3-4 STRESS THROUGH THICKNESS Model #5



Model 4 Adherend Lay-Up $(0_3/+45_3/90_3)_S$

Model 5 Adherend Lay-Up $(+45_3/0_3/90_3)_S$

Figure 3-5 LOCATION OF STRESS PLOTS

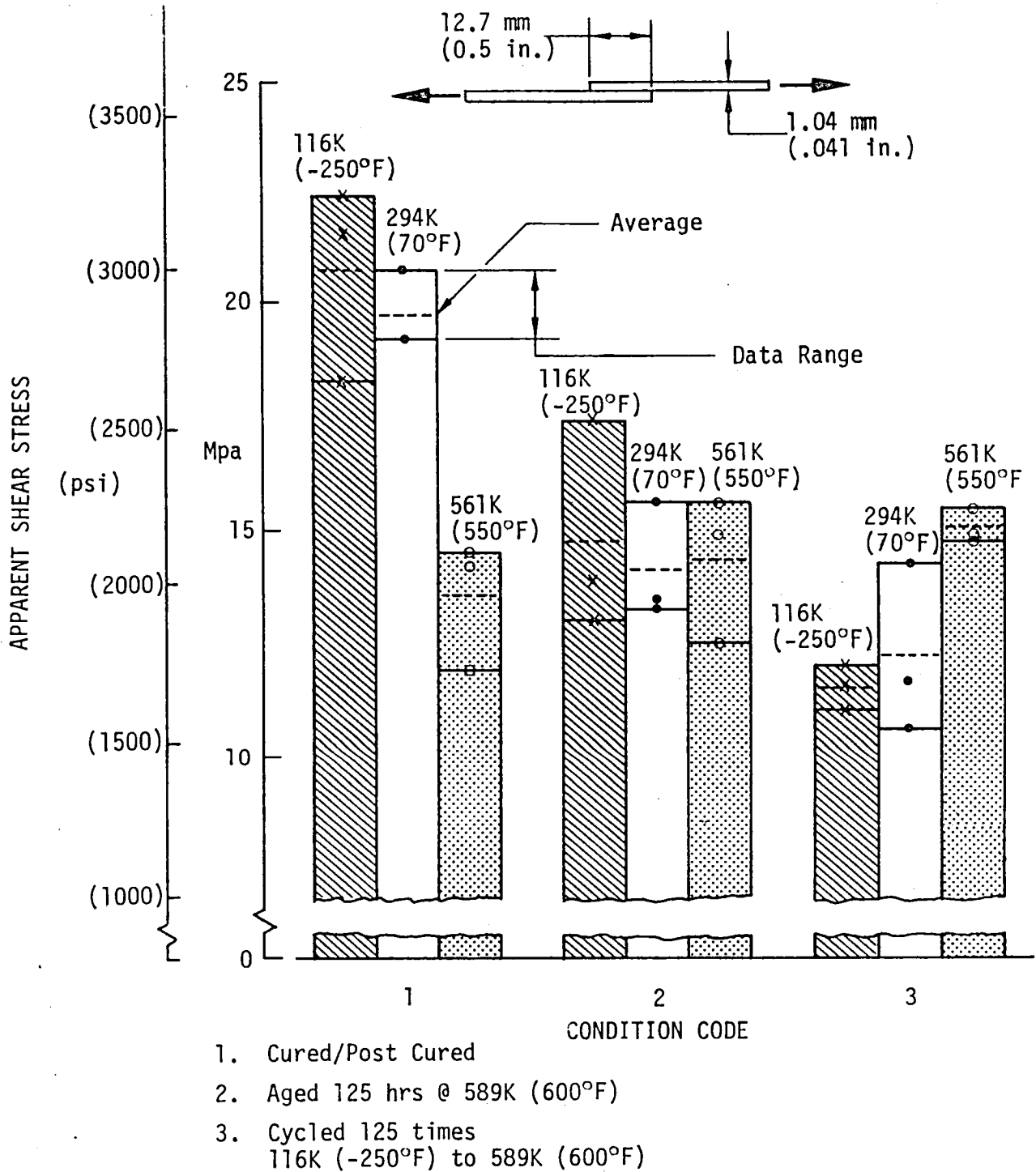


Figure 3-6: Matrix 2, Test 3, 12.7mm (0.50 in), Single Lap Titanium/Titanium, 1.04 mm (.041 in) Adherends A7F Adhesive

Table 3-1: Mechanical Properties of A7F
Cured/Post Cured Adhesive at 116K (-250°F)

SPECIMEN NO.	ULT. SHEAR STRENGTH Mpa/(psi)	SHEAR MODULUS Mpa/(psi)	ULT. SHEAR STRAIN
20	--	61.83/(8968)	--
23	--	--	--
24	25.11/(3643)	--	0.7085
21	20.02/(2904)	--	--

Table 3-2: Mechanical Properties of A7F
Cured/Post Cured Adhesive at 294K (70°F)

SPECIMEN NO.	ULT. SHEAR STRENGTH Mpa/(psi)	SHEAR PROP. LIMIT Mpa/(psi)	SHEAR MODULUS Mpa/(psi)	ULT. SHEAR STRAIN
13	16.60/(2407)	10.64/(1543)	71.51/(10,371)	0.3904
14	16.48/(2390)	8.52/(1236)	69.14/(10,027)	0.3758
15	17.09/(2479)	6.21/(900)	70.47/(10,221)	0.4337

Table 3-3: Mechanical Properties of A7F
Cured/Post Cured Adhesive at 561K (550°F)

SPECIMEN NO.	ULT. SHEAR STRENGTH Mpa/(psi)	SHEAR PROP. LIMIT Mpa/(psi)	SHEAR MODULUS Mpa/(psi)	ULT. SHEAR STRAIN
17	11.07/(1605)	3.88/(563)	45.49/(6597)	0.4375
18	8.34/(1209)	--	--	0.4311
19	6.98/(1012)	2.24/(326)	46.15/(6693)	0.4144

Table 3-4: Mechanical Properties of A7F Adhesive,
Conditioned at 600°F for 125 hours, at 116K (-250°F)

SPECIMEN NO.	ULT. SHEAR STRENGTH Mpa/(psi)	SHEAR MODULUS Mpa/(psi)	ULT. SHEAR STRAIN
2-20	21.71/(3149)	45.08/(6539)	0.6645
2-23	21.73/(3151)	35.31/(5121)	0.6429
2-24	20.18/(2927)	41.78/(6059)	0.5842

Table 3-5: Mechanical Properties of A7F Adhesive,
Conditioned at 600°F for 125 hours, at 294K (70°F)

SPECIMEN NO.	ULT. SHEAR STRENGTH Mpa/(psi)	INITIAL SHEAR MODULUS Mpa/(psi)	SECONDARY SHEAR MODULUS Mpa/(psi)	SHEAR PROP. LIMIT (mpa/(psi))	ULT. SHEAR STRAIN
2-13	18.60/(2697)	137.5/(19,938)	70.0/(10,156)	3.57/(518.7)	0.5320
2-14	13.13/(1904)	49.2/(7,138)	46.1/(6,688)	4.02/(583.9)	0.4975
2-15	16.12/(2399)	53.1/(7,701)	44.5/(6,448)	5.71/(827.6)	0.5495

Table 3-6: Mechanical Properties of A7F Adhesive,
Conditioned at 600°F for 125 hours, at 561K (550°F)

SPECIMEN NO.	ULT. SHEAR STRENGTH Mpa/(psi)	SHEAR PROP. LIMIT Mpa/(psi)	SHEAR MODULUS Mpa/(psi)	ULT. SHEAR STRAIN
2-16	12.82/(1859)	4.29/(623)	42.54/(6170)	0.4377
2-17	13.05/(1893)	3.30/(479)	67.63/(9808)	0.3729
2-18	14.12/(2048)	4.94/(717)	47.93/(6951)	0.5271

post-cured specimens. Test results are shown in Figure 3-7. All specimens failed cohesively.

Stainless steel bars were bonded with A7F adhesive and heat aged [125 Hrs @ 589°K (600°F)] to complete the Matrix 2 Test 5 specimens. After aging the specimens showed severe heat degradation or some type of reaction between the stainless steel and the adhesive. Seven specimens had failed in the oven and the remaining specimens were not tested. A second test of specimens were bonded and aged and experienced the same failures. The stainless steel bars were replaced with titanium and new specimens made. Test results are shown in Figure 3-7. All specimens failed cohesively.

Attempts to compression mold a "neat" adhesive (A7F) tension test specimen for Matrix 2, Test 1 were unsuccessful. The molds experienced some leakage during resin B-staging; however, the major problem was fracture of the brittle adhesive during cool-down and subsequent removal from the mold. The molded sheet would have to have undergone additional machining and handling after removal from the mold. Because of the brittle nature of the adhesive, there was a high probability there would be significant breakage during these operations. The decision was reached to not expend additional resources because of the low probability of success. Program schedules and costs prevent trying an alternate test procedure. Flatwise tension ultimate of the A7F under a constrained condition, Matrix 2 Test 5, will be used for analysis purposes.

3.1.3 TASK 2.1.4 - Joint Specimen Fabrication and NDE

A summary of specimens fabricated through this reporting period is given in Table 3-7. All the Matrix 2 and Matrix 3 series specimens have been fabricated. Remaining specimens for Matrix 1 and 4 are those requiring honeycomb core.

Honeycomb core was received in-house on September 22, 1980. The first sandwich panels to be made were for the Matrix 1 sandwich beam specimen; however, the core crushed during autoclave cure at .69 MPa (100 psi) and 589°K (600°F). Investigation into the cause revealed that the core received had not been post-cured. All the core was returned to the vendor to be post-cured and is scheduled to be returned by November 21, 1980.

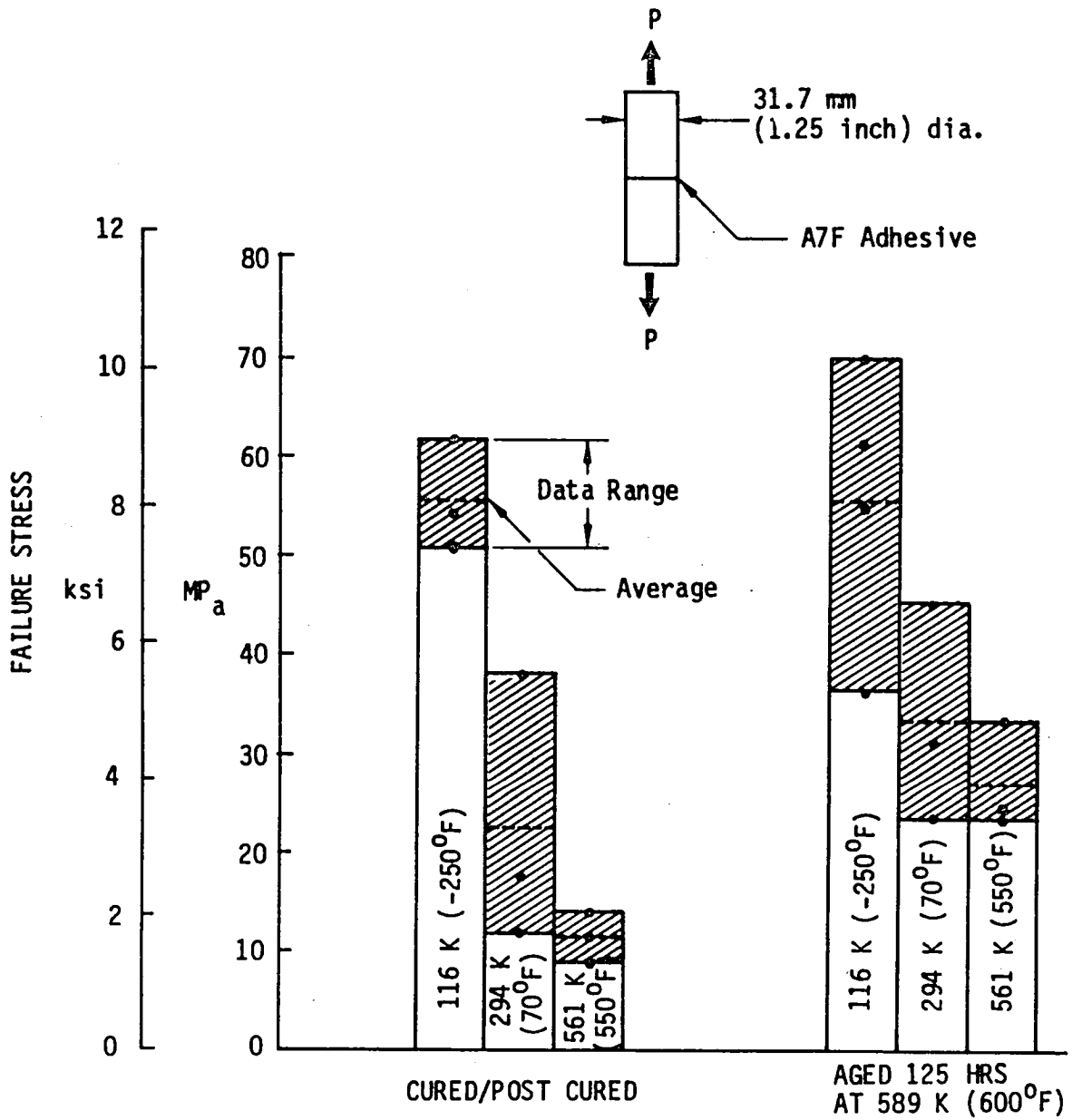


Figure 3-7 Flatwise Tension A7F Adhesive Matrix 2 Test 5

Table 3-7 Specimen Fabrication and Test Summary
GR/PI Joint Contract NAS1-15644

TEST	MATRIX NO.	NO. OF PANELS		NO. OF SPEC.	
		REQ'D.	MADE	REQ'D.	MADE
DESIGN ALLOWABLES	1	16	16	226	175
ANCILLARY ADHESIVE	2	N/A	N/A	63	54
STANDARD JOINT	3A	18	18	126	124
	3B	3	3	54	54
	3C	2	2	6	6
	3D	44	44	192	192
	3E	6	6	54	54
	3F	4	4	12	12
	3G	INTEGRAL LAYUP		54	54
SMALL SPECIMENS	4A	12	12	72	71
	4B	21	21	60	30
	4C	27	27	18	6

N/A = NOT APPLICABLE

All the Matrix 3G "3-step" specimens had good bonds (no voids); however, all the "5-step" specimens had bondline voids. The voids were indicated by the panel C-scans and could be visually seen on the edges of the cut specimens. It is expected that the bondline voids were caused by volatiles not being able to escape through the thicker laminate of the "5-step" joint as compared to the "3-step" joints. Costs and schedules preclude remaking these specimens.

3.1.4 TASK 2.1.5 - Standard Joint Tests

All of the Matrix 3 series of Standard Joint Tests have been completed. These tests were to establish a data base and to evaluate effects of various parameters on the performance of single lap, double lap and symmetric step-lap bonded joints. Parameters investigated were lap length, temperature, adherend stiffness, laminate stacking and adherend tapering. A total of 496 specimens were tested. Test matrices are given in Reference 4. Analysis and discussion of test results are presented in Section 3.1.5.

The Matrix 3G "5-step" specimens, Tests 3G-1b and 3G-2a, had bondline voids and delaminations which precluded meaningful test results. These specimens were tested at room temperature only and then examined to try and relate actual bondline voids with those indicated by the "C-scans". The "3-step" specimens had clear "C-scans" and were tested as planned.

3.1.5 TASK 2.1.6 - Test Analysis and Correlation

Test results obtained for the single and double lap joints had a significant amount of data scatter. It is felt that the large scatter is primarily due to processing and manufacturing variables. To establish a feel for the quality of the data, standard deviations and coefficients of variation were calculated for all the test results. Coefficients of variation for the single lap joints range from 0.047 to 0.41 and for the double lap joints from 0.023 to 0.355. The "3 step" symmetric step lap joints had coefficients of variation from 0.032 to 0.087. In all cases the joints experienced an interlaminar composite failure at the joint interface. There were no adhesive failures. The large data scatter preclude doing a meaningful correlation of all the test results; therefore, analysis correlation efforts are aimed at identifying and predicting behavioral trends observed based on averages.

A summary of trends observed for all the various parameters tested is given in Tables 3-8 through 3-11. Areas that are crosshatched represent trends that are the opposite of what would be expected based on theoretical considerations. There are no apparent explanations for these other than processing and material variables.

To be more structurally efficient, the double lap joint should more than double the strength of a single lap joint with the same bonded lap length. Failure loads for single and double lap joints versus lap length are given in Figures 3-8 through 3-10. These figures show that the double lap joint failure load is 3 to 4 times greater than the same length single lap joint. Structural efficiencies of GR/PI to GR/PI single lap joints varied from .118 to .264 and for double lap joints from .178 to .424. Efficiencies of GR/PI to titanium single lap joints varied from .135 to .382 and for double lap joints from .238 to .619. The greater efficiency of the double lap joints is because the load eccentricity and corresponding moment is eliminated due to joint symmetry. Increasing the extensional stiffness of the joint increased its load carrying capability; however, there was no significant change in the joint efficiency since the basic adherend strength also increased.

Test results have been plotted showing average failure load (nominally of 6 data points) versus the various parameters tested. These data are presented to allow a quick perusal of test trends and are described below.

In all cases the joints failed due to interlaminar shear and peel. There were no adhesive failures except for a few GR/PI to titanium joints. These had some evidence of cohesive failure, but the area involved was a very small percentage of the total bonded area.

Effects of temperature and lap length for GR/PI to GR/PI single lap joints are shown in Figure 3-11. Similar data for GR/PI to Titanium single lap joints are shown in Figure 3-12. Differences in coefficients of thermal expansion (CTE) of joint materials cause thermal stresses to develop in the joint when it is cured at elevated temperature (stress free state) and then cooled to ambient. When the joints are tested at elevated temperature the thermal stresses are relieved resulting in higher failure loads. This trend is shown by the data given in Figures 3-11 and 3-12. It is more pronounced for GR/PI to Titanium (Figure 3-12) because of large differences in CTE's. Slight softening of the

Table:3-8 Standard Joint Summary Trends Observed (Averages) Single Lap Joint

(read down only)

PARAMETER	116°K (-250°F)	294°K (70°F)	561°K (+550°F)
Increase Lap Length 12.7mm 0.5 inch 25.4mm (1.0 Inch) 50.8mm (2.0 Inch) 76.2mm (3.0 Inch)	Ref	Ref	Ref
	DEC	INC	INC
	INC	INC	INC
	INC	INC	INC
Stacking @ Interface 00 +450 03	Ref	Ref	Ref
	NT	INC	NT
	NT	INC	NT
Increase Axial Stiff (3A-1b Ref)	INC	INC	INC
Bending Stiffness (3A-1b Ref) Increase Decrease	NT	INC	NT
	NT	INC	NT
Stiffness Imbalance (3A-1b Ref)	DEC	DEC	INC
Tapering (3A-6a Ref)	NT	INC	NT
Titanium (Compared to GR/PI) 25.4mm (1.0 Inch) 50.8mm (2.0 Inch) 76.2mm (3.0 Inch)	INC	DEC	0
	0	INC	INC
	DEC	DEC	INC
Titanium increase lap length 25.4mm (1.0 Inch) 50.8mm (2.0 Inch) 76.2mm (3.0 Inch)	Ref	Ref	Ref
	INC	INC	INC
	INC	INC	INC

LEGEND:
 0 = no change in load
 INC = increase in load
 DEC = decrease in load
 NT = not tested

Table:3-9 Standard Joint Summary Trends Observed Due to Temp Change (Based on Averages)

Single Lap Joint

(read across only)

TEST NO.	116°K (-250°F)	294°K (700°F)	561°K (550°F)
3A-1a	DEC	REFERENCE	INC
1b	0		INC
1c	0		INC
2a	INC		INC
3a	NT		NT
4a	NT		NT
5a	DEC		INC
6a	NT		NT
7a	INC		INC
3B-1a	DEC		INC
1b	DEC		INC
1c	DEC		INC
3C-1a	NT	REFERENCE	NT

LEGEND:

- 0 = no change in load
- DEC = decrease in failure load
- INC = increase in failure load
- NT = not tested

Table:3-10 Standard Joint Summary Trends Observed Due to Temp Change - Based on Averages.

Double Lap Joint

(read across only)

TEST NO.	116°K (-250°F)	294°K (70°F)	561°K (550°F)
3D-1a	INC	REFERENCE	INC
1b	INC		INC
1c	0		INC
2a	DEC		INC
2b	INC		DEC
2c	DEC (SLIGHT)		INC
3a	0		INC
4a	DEC		INC
5a	INC		INC
6a	INC		INC
7a	NT		INC
3E-1a	DEC		DEC
1b	DEC		INC
2a	DEC		INC
3F-1a	NT		0
3G-1a	DEC		INC
1b	NT		NT
2a	NT	REFERENCE	NT

LEGEND:

- 0 = no change in load
- DEC = decrease in failure load
- INC = increase in failure load
- NT = not tested

Table: 3-11 Standard Joint Summary Trends Observed (Averages) Double Lap Joint
(read down only)

PARAMETER	116°K (-250°F)		294°K (700°F)		561°K (550°F)	
	1mm/2mm* (.04"/.08")	1.5mm/3.0mm* (.06"/.12")	1mm/2mm* (.04"/.08")	1.5mm/3.0mm* (.06"/.12")	1mm/2mm* (.04"/.08")	1.5mm/3.0mm* (.06"/.12")
Increase Lap Length 20.3mm (0.8 inch) 33.0mm (1.3 Inch) 45.7mm (1.8 Inch)	Ref	Ref	Ref	Ref	Ref	Ref
	DEC	INC	INC	INC	INC	INC
	DEC	INC	0	INC	DEC	INC
Stacking @ Interface 3D-2b Ref. +45° 0 ₃ °	0		0		INC	
	DEC		DEC		INC	
Increase Axial Stiffness 3D-2b Ref.	0		INC		INC	
Bending Stiffness 3D-2b Ref. Increase Decrease	DEC		DEC		INC	
	0		0		INC	
Stiffness Imbalance 3D-2b Ref.	DEC		DEC		DEC	
Tapering (3D-7a Ref.)	NT		INC		INC	
Titanium (Compared to Graphite) Lap Length 20.3mm (0.8 Inch) 45.7mm (1.8 Inch)	INC		INC		INC	
	DEC		DEC		INC	
Titanium Increase Lap Length 20.3mm (0.8 Inch) Ref. 45.7mm (1.8 Inch) 45.7mm (1.8 Inch) Ref. +45°	DEC		DEC		INC	
	INC		DEC		INC	

*outer adherend thickness/inner adherend thickness

LEGEND:

0 = no change in load
INC = increase in load
DEC = decrease in load
NT = not tested

- × Double Lap
- Single Lap

1.52 mm (.06 inch) adherends Average of 6 Data Points

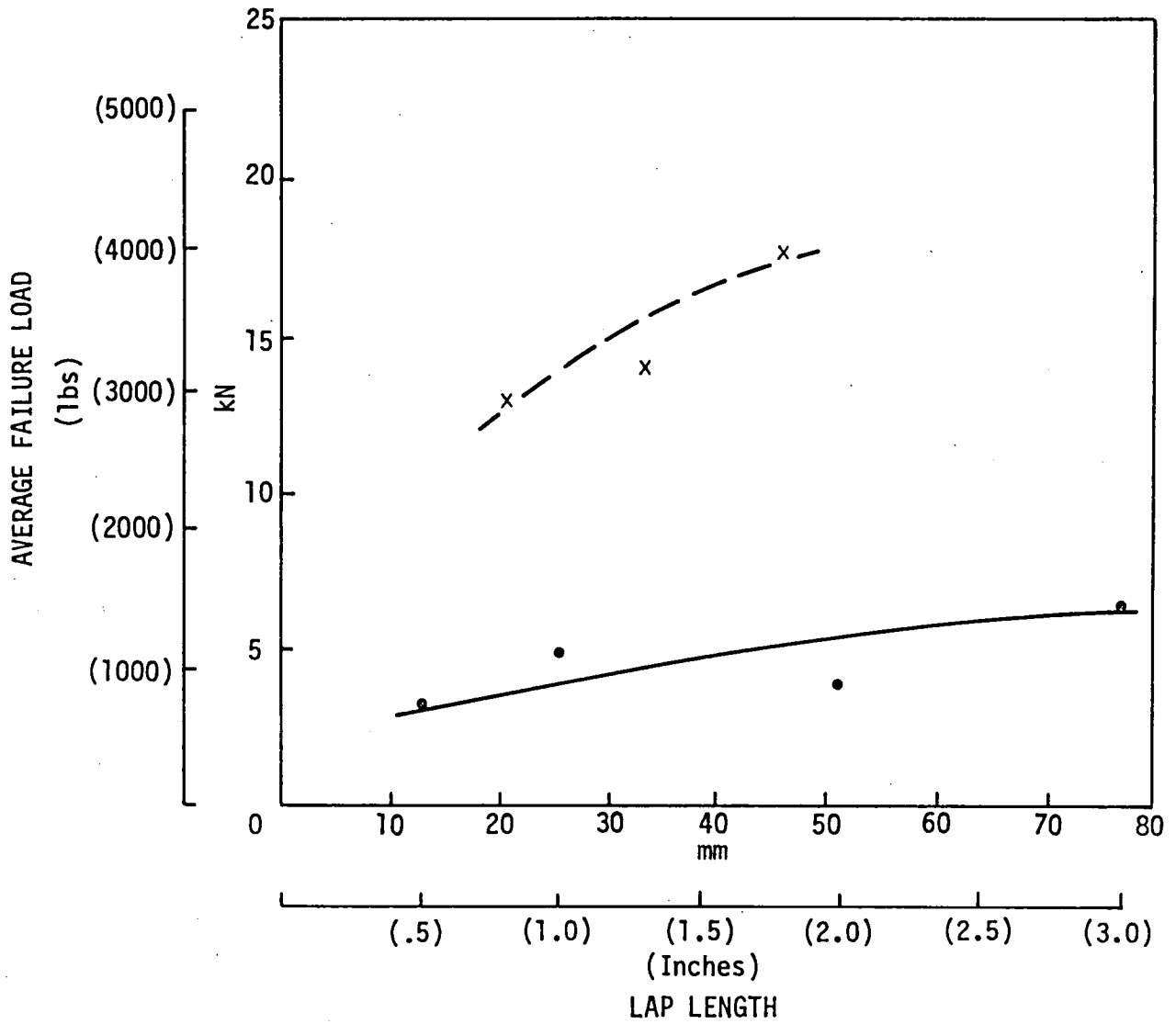


FIGURE 3-8 Comparison of Double & Single Lap Joints at 561°K (550°F)

x Double Lap
• Single Lap

1.52 mm (.06 inch) adherends Average of 6 Data Points

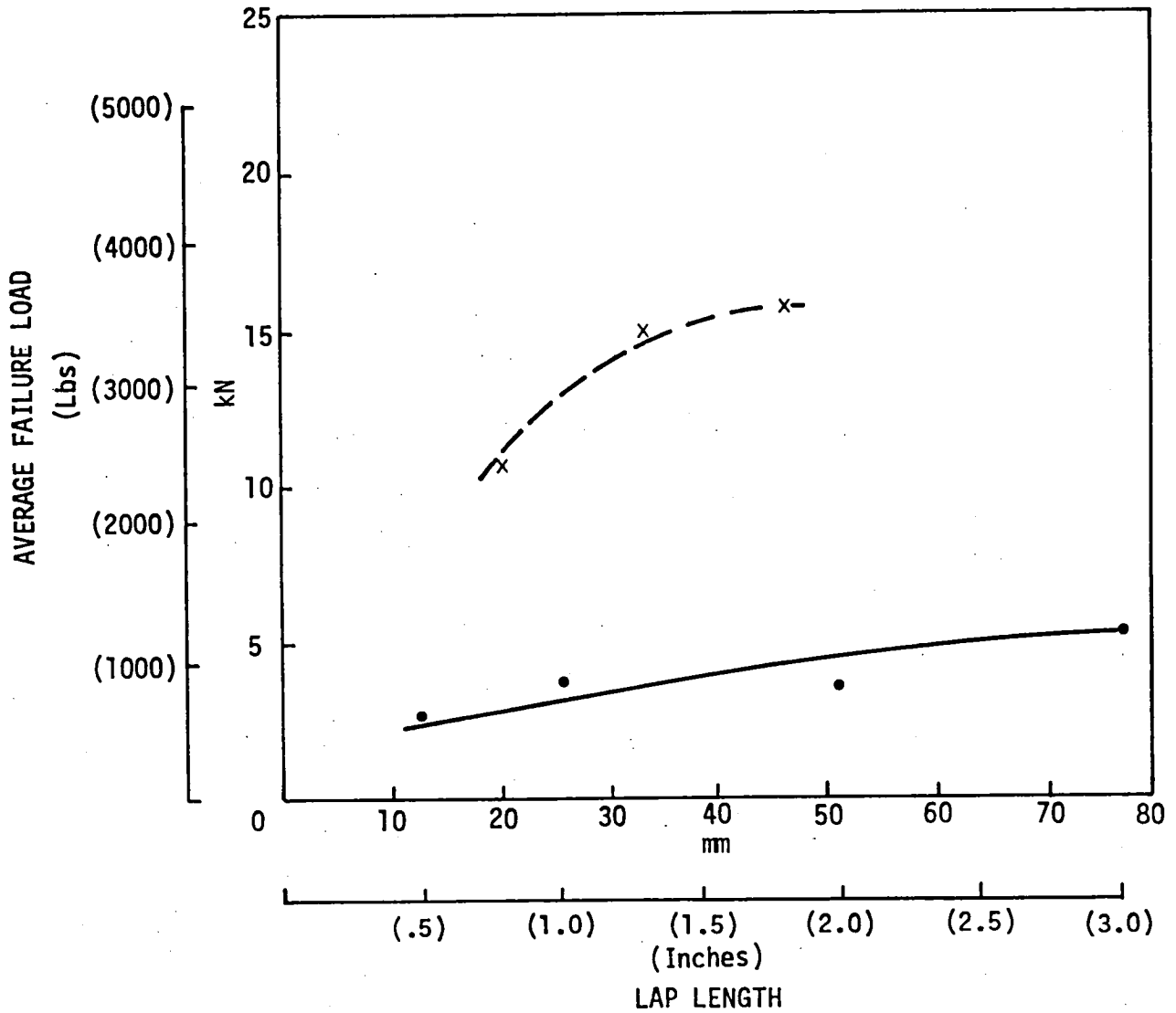


FIGURE 3-9 Comparison of Double & Single Lap Joints at 294°K (70°F)

- x Double Lap
- Single Lap

1.52 mm (.06 inch) Adherends

Average of 6 Data Points

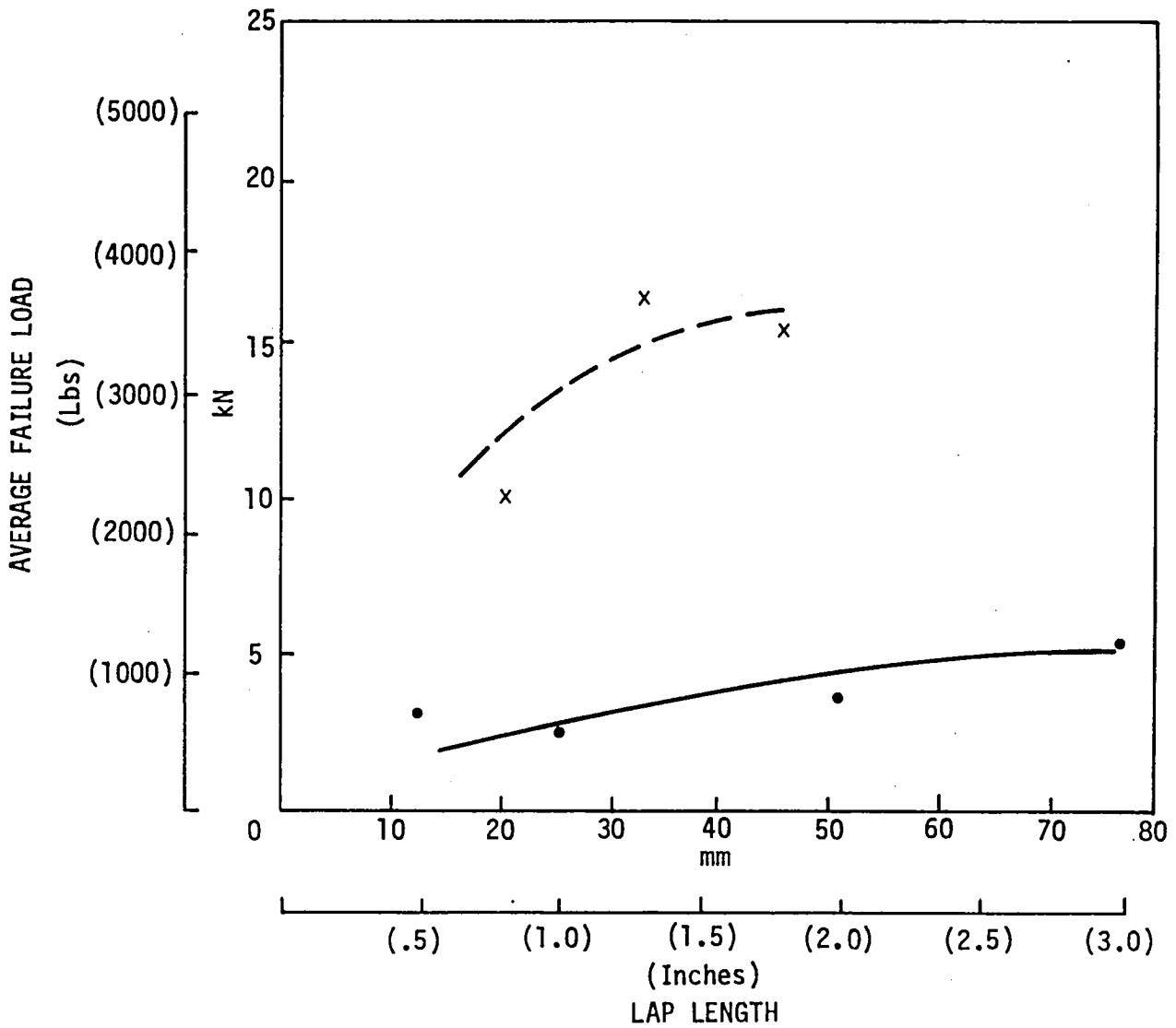


FIGURE 3-10 Comparison of Double & Single Lap Joints at 116°K (-250°F)

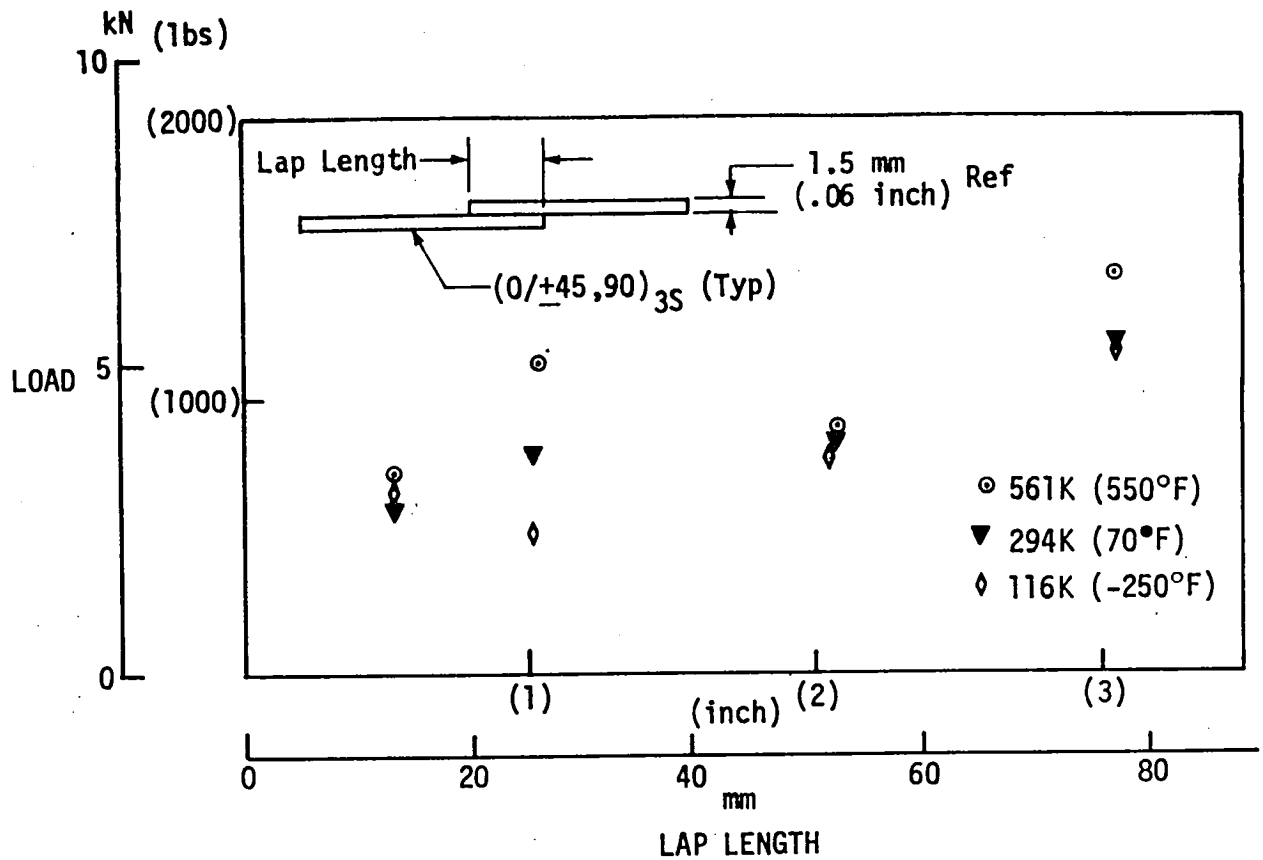


Figure 3-11 Average Failure Load vs Lap Length-Graphite/Polyimide Single Lap Joint - Celion 3000/PMR-15, A7F Adhesive

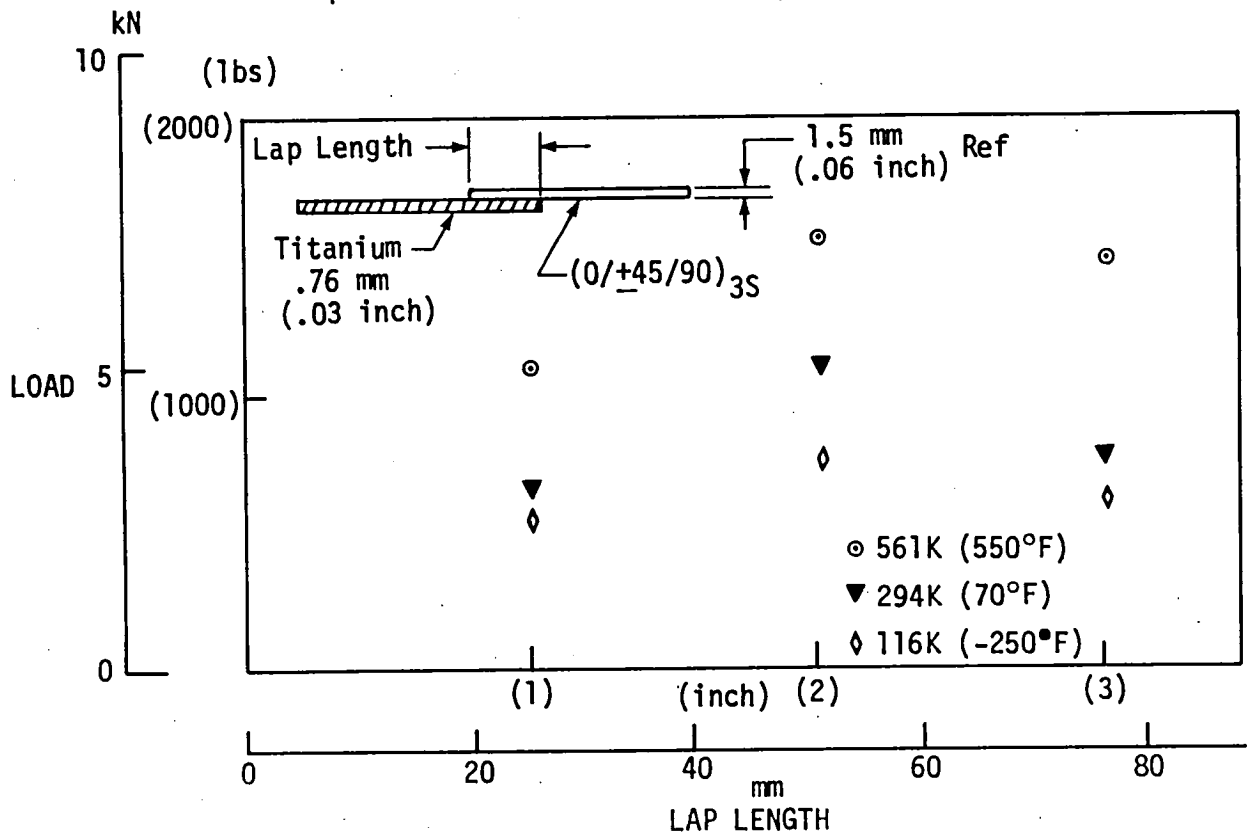


Figure 3-12 Average Failure Load vs Lap Length Graphite/Polyimide to Titanium-Single Lap Joint - Celion 3000/PMR-15, A7F Adhesive

adhesive and fiber matrix at elevated temperature would make the joint more ductile and also contribute to the increase in joint strength. Increasing the lap length also increases the failure load, but only up to some maximum length beyond which there is no additional increase.

Increasing the axial and bending stiffness of the adherends, for the same thickness, resulted in a significant increase in failure load as shown in Figure 3-13. Testing of an unbalanced joint (different adherend thicknesses) showed a reduction in joint strength (see Figure 3-14), except at 561K (550°F). There was no significant change at elevated temperature.

Other parameters tested were effects of tapering the adherend to reduce peel stresses and of varying the laminate stacking sequence. Tapering the adherend on a GR/PI to GR/PI 50.8 mm (2.0 inch) single lap joint with 2.54 mm (.10 inch) thick adherend showed a 23.7 percent increase in failure load as compared to no tapering (tested at room temperature).

The baseline single lap joint has adherends of $(0/+45/90)_{3S}$ laminates. Two other laminates were tested to evaluate the effect of ply stacking sequence at the bondline interface. Laminate layups tested were $(0_3/+45_3/90_3)_S$ and $(+45/0/90)_{3S}$ with 50.8 mm (2.0 inches) lap length. In both cases the average failure load was increased over the baseline by 49%.

Results for double lap joints are shown in Figures 3-15 through 3-20. GR/PI to GR/PI double lap joints were tested for two combinations of adherend thicknesses. Results are shown in Figures 3-15 and 3-16. Results for GR/PI to Titanium double lap joints are shown in Figure 3-17. The predominate trend is an increase in failure load with temperature; however, as can be seen, there are some exceptions. These cannot be explained at this time, except as due to possible processing variables and data scatter. The increase in joint strength with temperature is attributed to the same reasons discussed for single lap joints above.

Joint failure theory predicts that a stiffness balanced joint is stronger than an unbalanced joint. This is demonstrated by the results in Figure 3-18. Likewise, increasing the axial and bending stiffness should increase the joint strength. Results in Figure 3-19 show this except at 116K (-250°F) there was no significant change.

Effects of different ply stacking sequences in the adherends is shown in Figure 3-20. The baseline had adherends with $(0/+45/90)_3S$ laminate. The other stackings tested were $(0_3/+45_3/90_3)_S$ and $(+45/0/90)_3S$. Finite element analyses were performed to evaluate the effect of the above ply stacking sequences on joint performance. Analysis results are presented in Ref. (3rd Quarterly).

Interpretation of the analysis results is dependent on knowing the failure initiation mode, i.e., is it due to shear stress or peel stress. If shear stresses dominate, then the $+45$ laminate should have the highest failure load. If peel stresses dominate, then the 0_3 laminate would have the highest failure load. Test results indicate that the $+45$ laminate is stronger than the 0_3 laminate in all cases; however, it had the same strength as the baseline laminate at 116K (-250°F) and room temperature. The 0_3 laminate is weaker than the baseline at 116K (-250°F) and room temperature and stronger at 561K (550°F). This would indicate that the failures are being initiated by shear stresses rather than peel stresses; however, there are insufficient data to draw firm conclusions at this time.

Results for the "3 step" symmetric step-lap joint are given in Figure 3-21. Failure loads for the joint were calculated for the 561K (550°F) test condition using computer code A4EGX. This code was developed by L. J. Hart-Smith of McDonnell-Douglas. Adhesive properties used in the analysis were those from the thick adherend tests conducted at the University of Delaware (see Section 3.1.2). The predicted failure load was 898 kN/m (5126 lbs/in), compared to an average failure load based on 6 data points of 901 kN/m (5147 lb/in). It must be noted, however, that the code predicted an adhesive failure, whereas the actual joints had interlaminar composite failures. Actual joints were co-cured onto the titanium steps using only an adhesive primer. They were not precured laminates bonded on with a separate adhesive. The analysis code requires adhesive thickness and properties as an input. The co-cured joints were simulated for analysis purposes by inputting adhesive properties and a thickness of 0.127 mm (.005 inch). Analyses were not conducted for room temperature and 116°K (-250°F) test conditions because of code problems encountered when a large temperature differential was input.

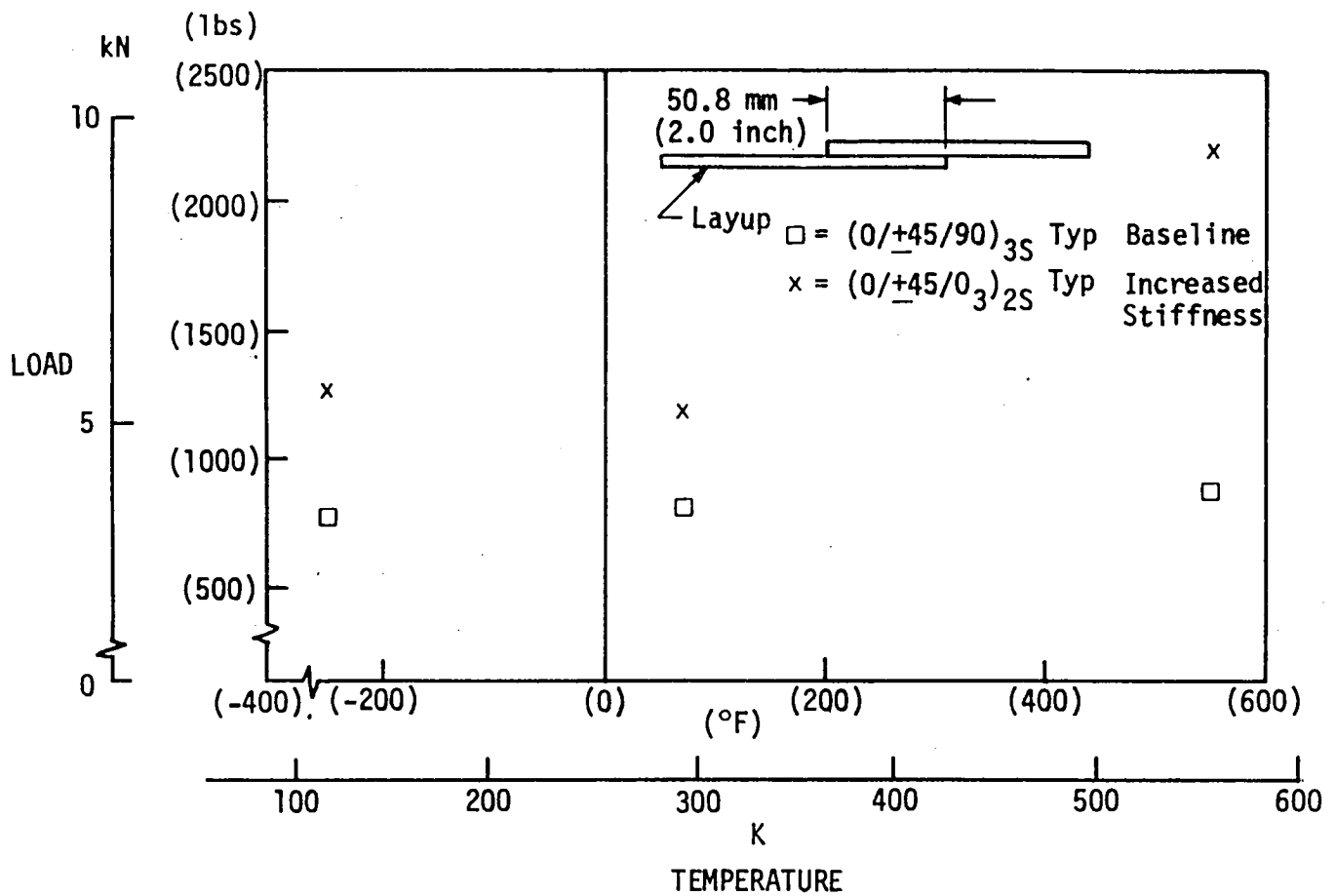


Figure 3-13 Average Failure Load vs Temperature-Effect of Increased Axial Stiffness- Graphite/Polyimide Single Lap Joint - Celion 3000/PMR-15, A7F Adhesive

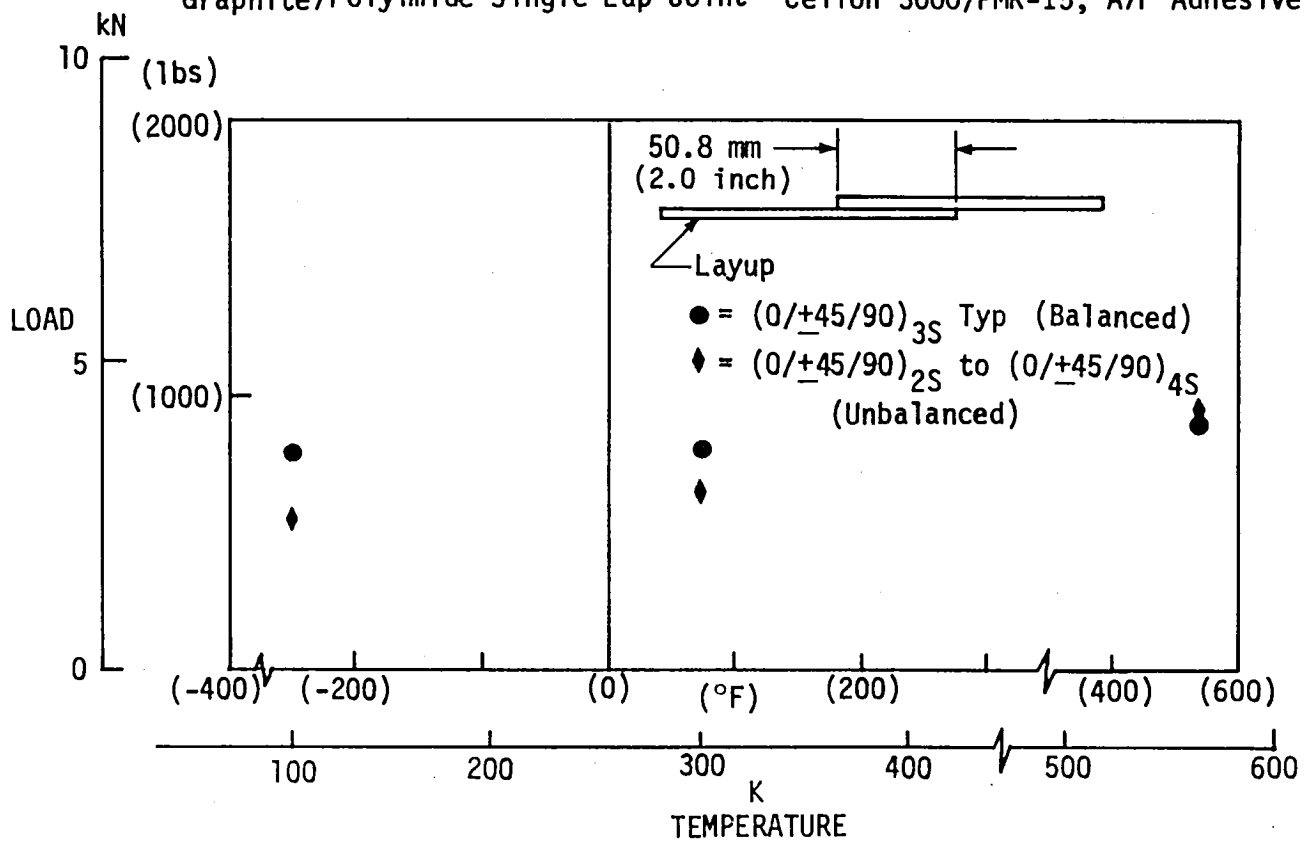


Figure 3-14 Average Failure Load vs Temperature-Effect of Stiffness Imbalance - Graphite/Polyimide Single Lap Joint - Celion 3000/PMR-15, A7F Adhesive

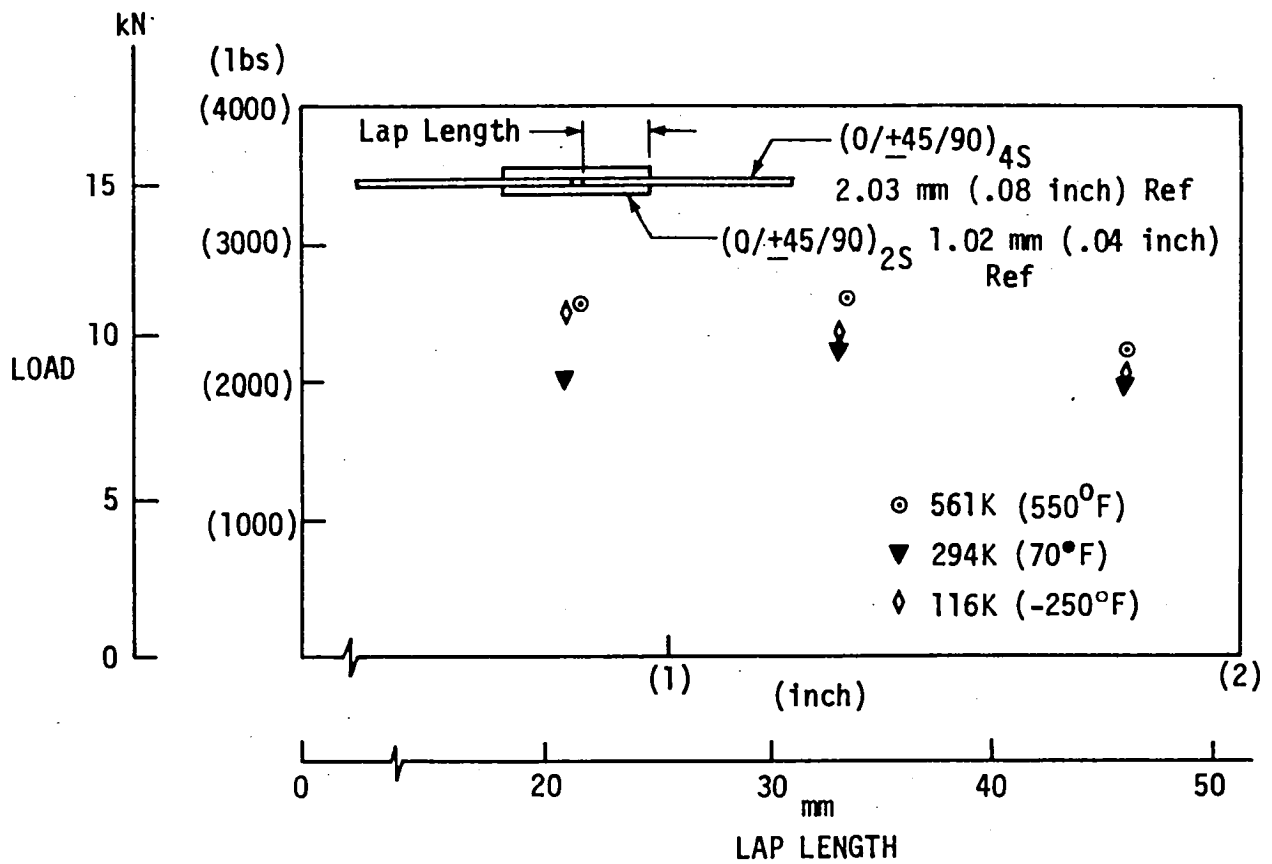


Figure 3-15 : Average Failure Load vs Lap Length- Graphite/Polyimide Double Lap Joint-Celion 3000/PMR-15, A7F Adhesive

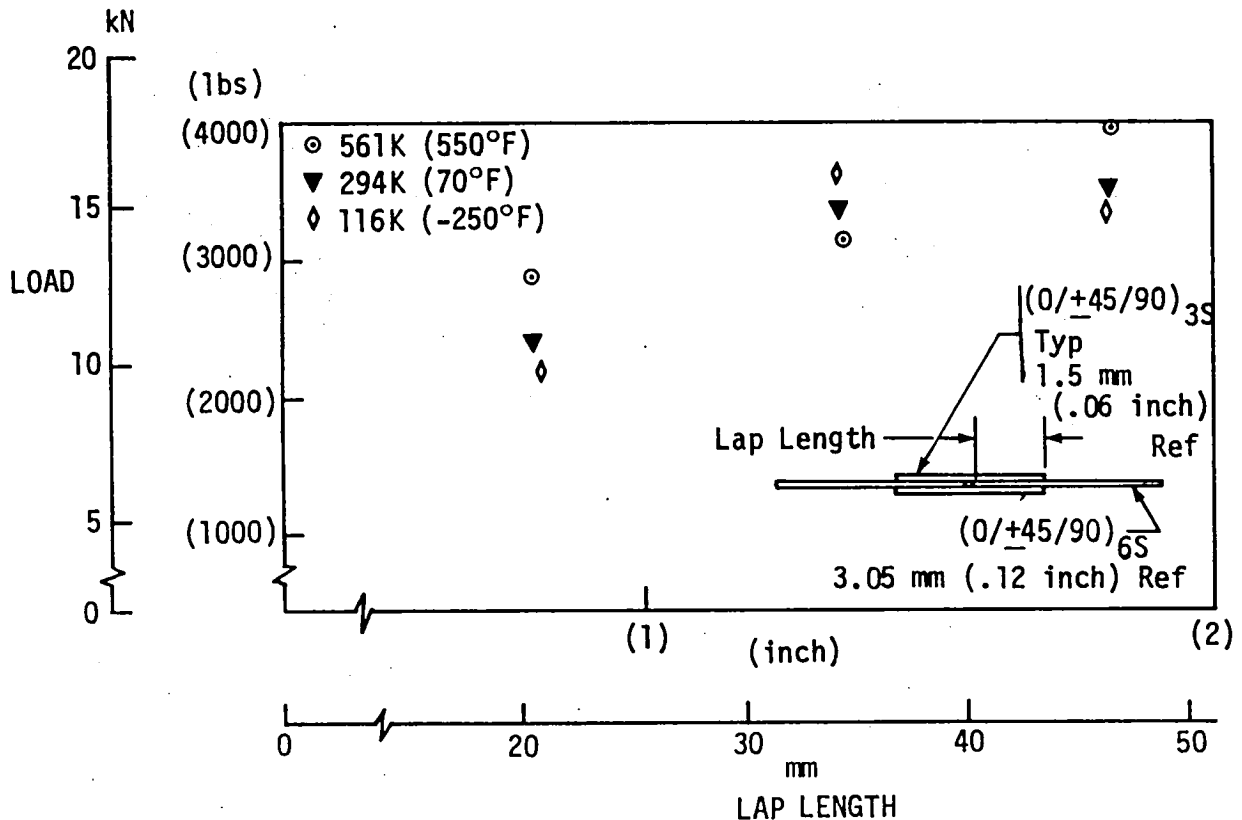


Figure 3-16 : Average Failure Load vs Lap Length-Graphite/Polyimide Double Lap Joint-Celion 3000/PMR-15, A7F Adhesive

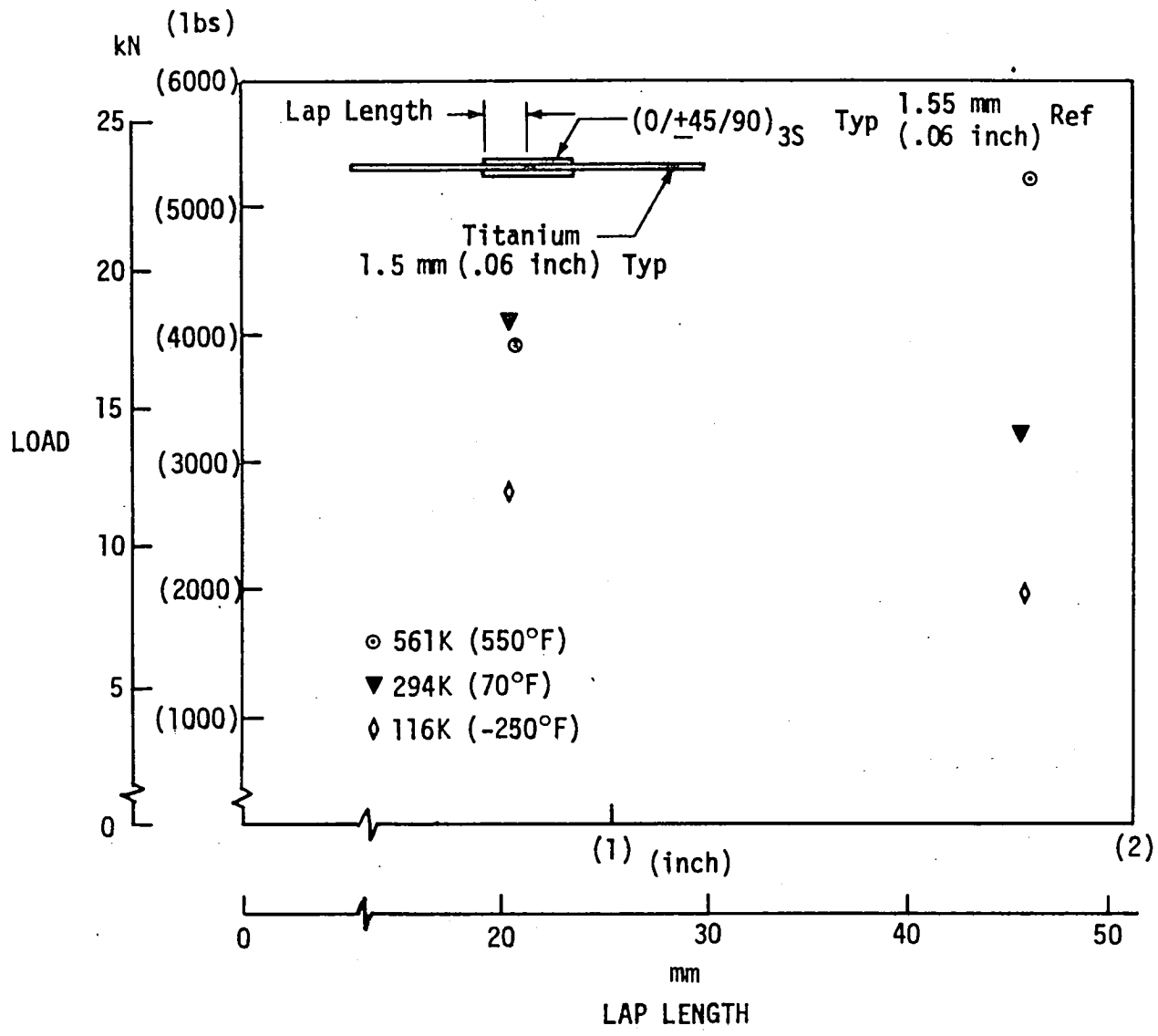


Figure 3-17 : Average Failure Load vs Lap Length-Graphite/Polyimide To Titanium- Double Lap Joint-Celion 3000/PMR-15, A7F Adhesive

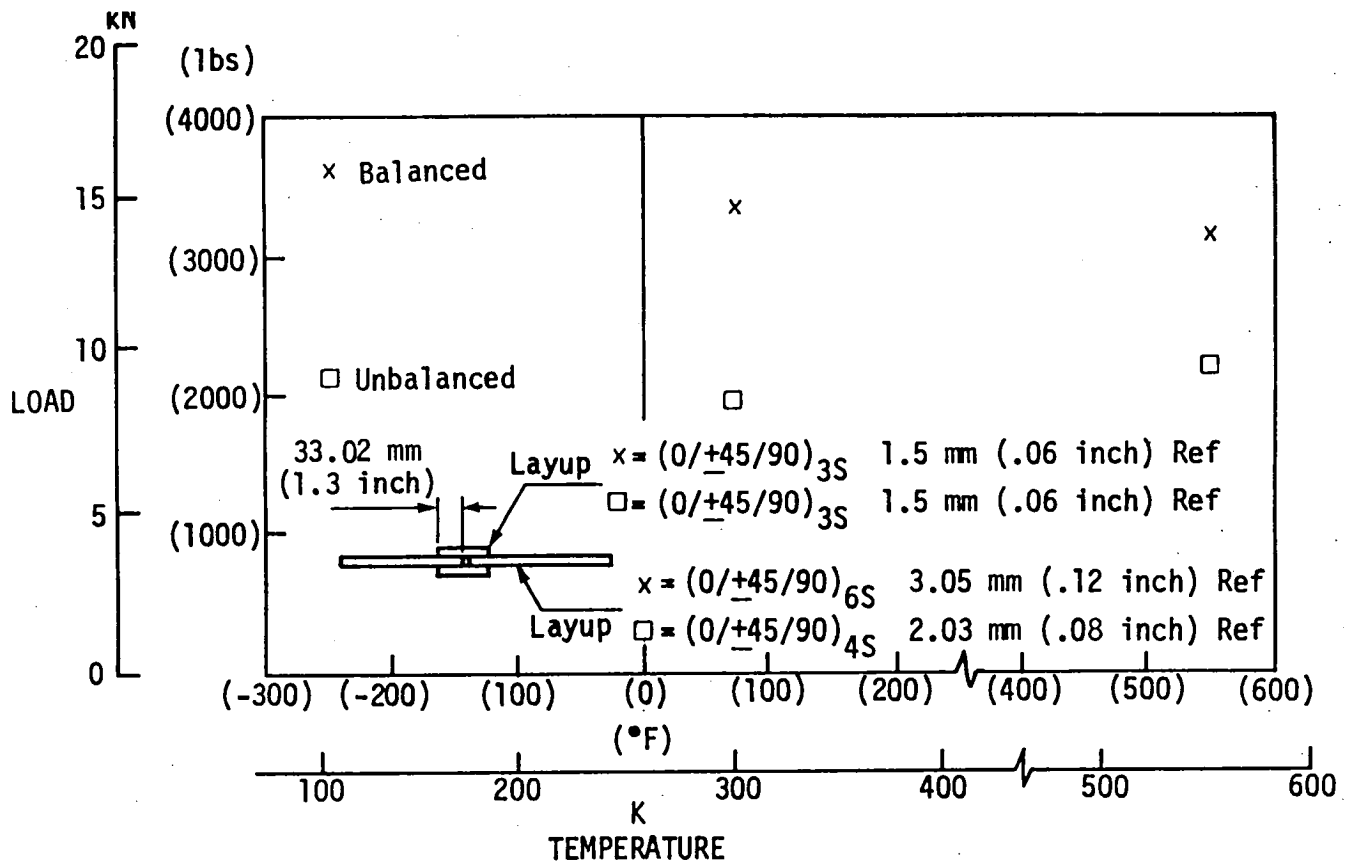


Figure 3-18 : Average Failure Load vs Temperature-Effect of Stiffness
Imbalance-Double Lap Joint-Celion 3000/PMR-15, A7F Adhesive

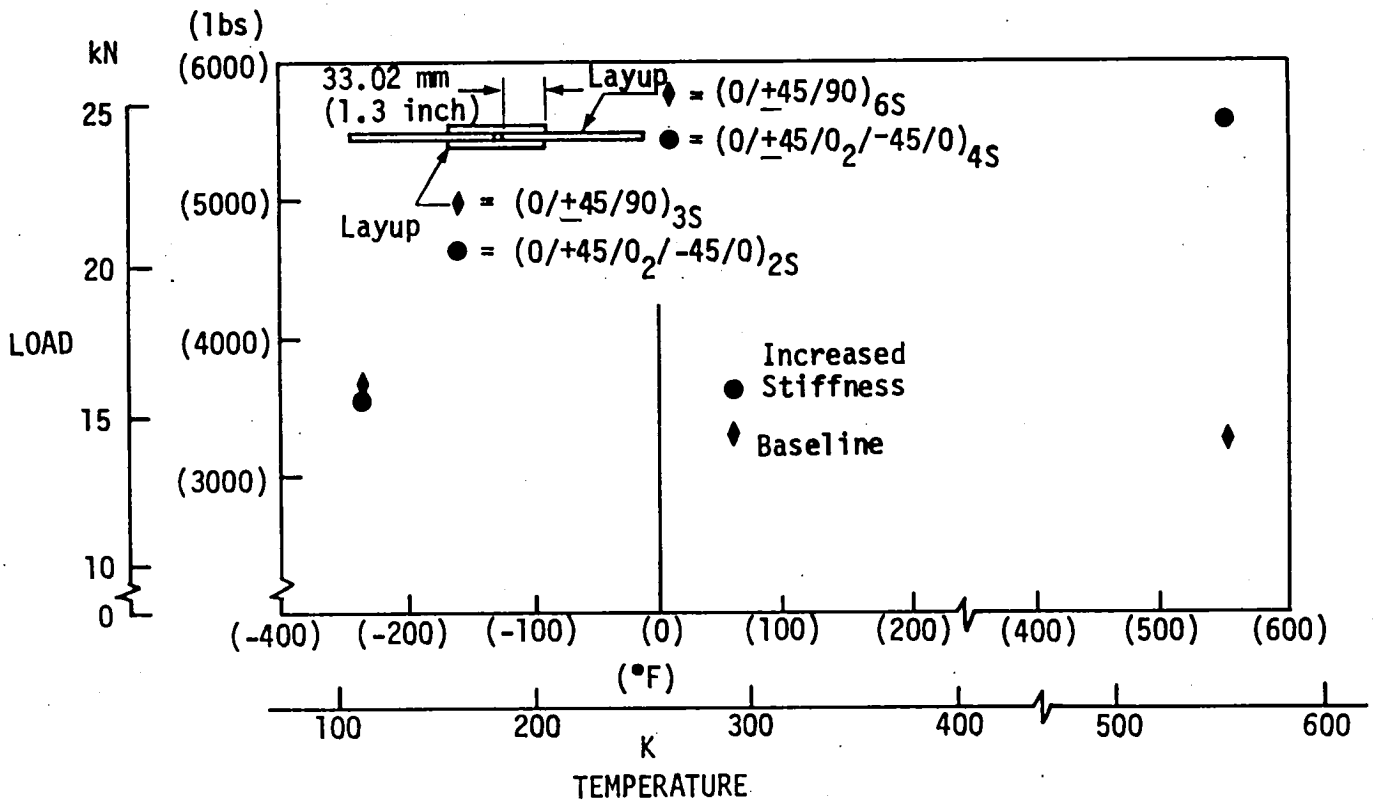


Figure 3-19 : Average Failure Load vs Temperature-Effect of Increased Axial
Stiffness - Graphite/Polyimide Double Lap Joint-
Celion 3000/PMR-15, A7F Adhesive

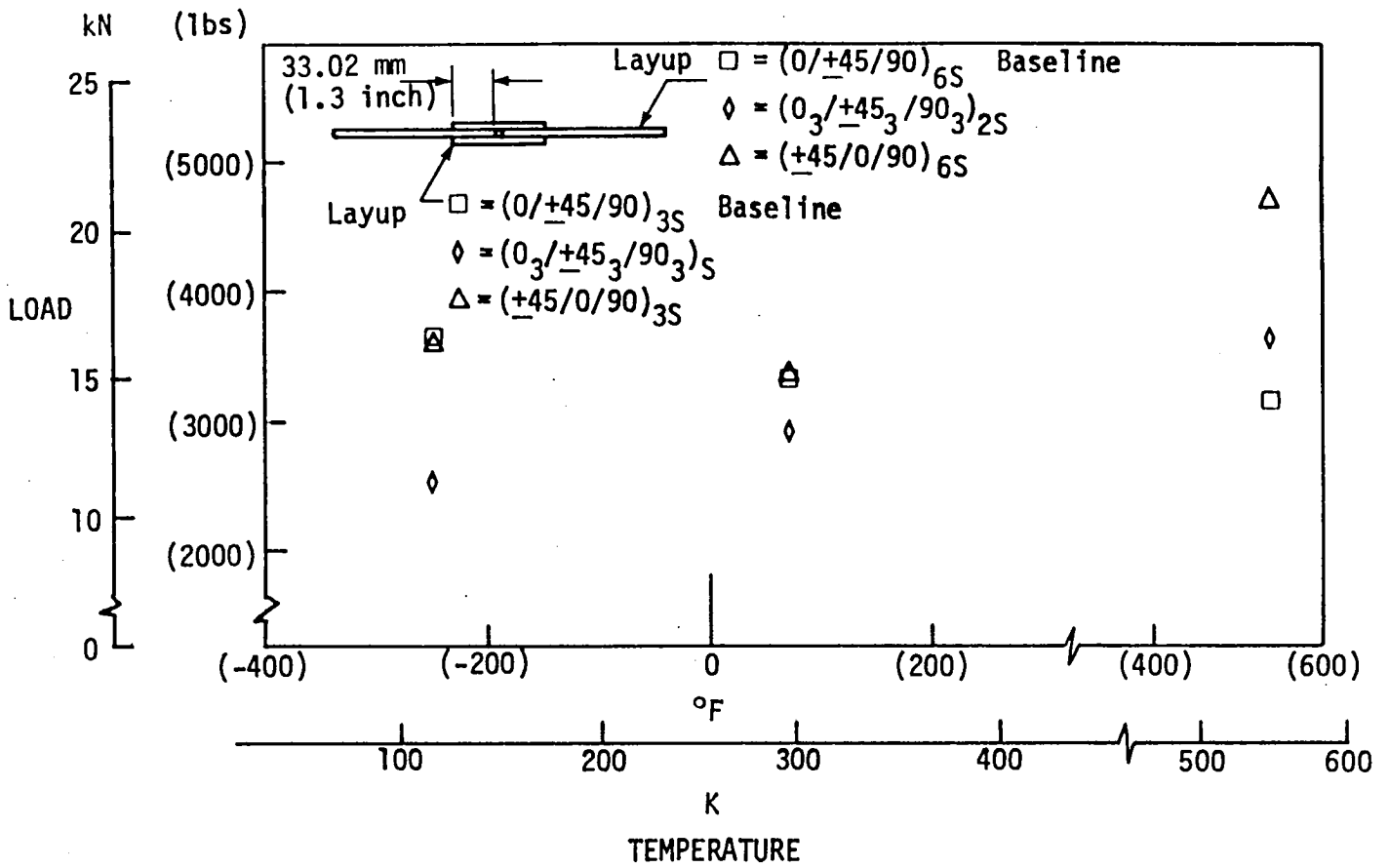


Figure 3-20: Average Failure Load vs Temperature-Effect of Ply Stacking Sequence - Double Lap Joint - Celion 3000/PMR-15, A7F Adhesive

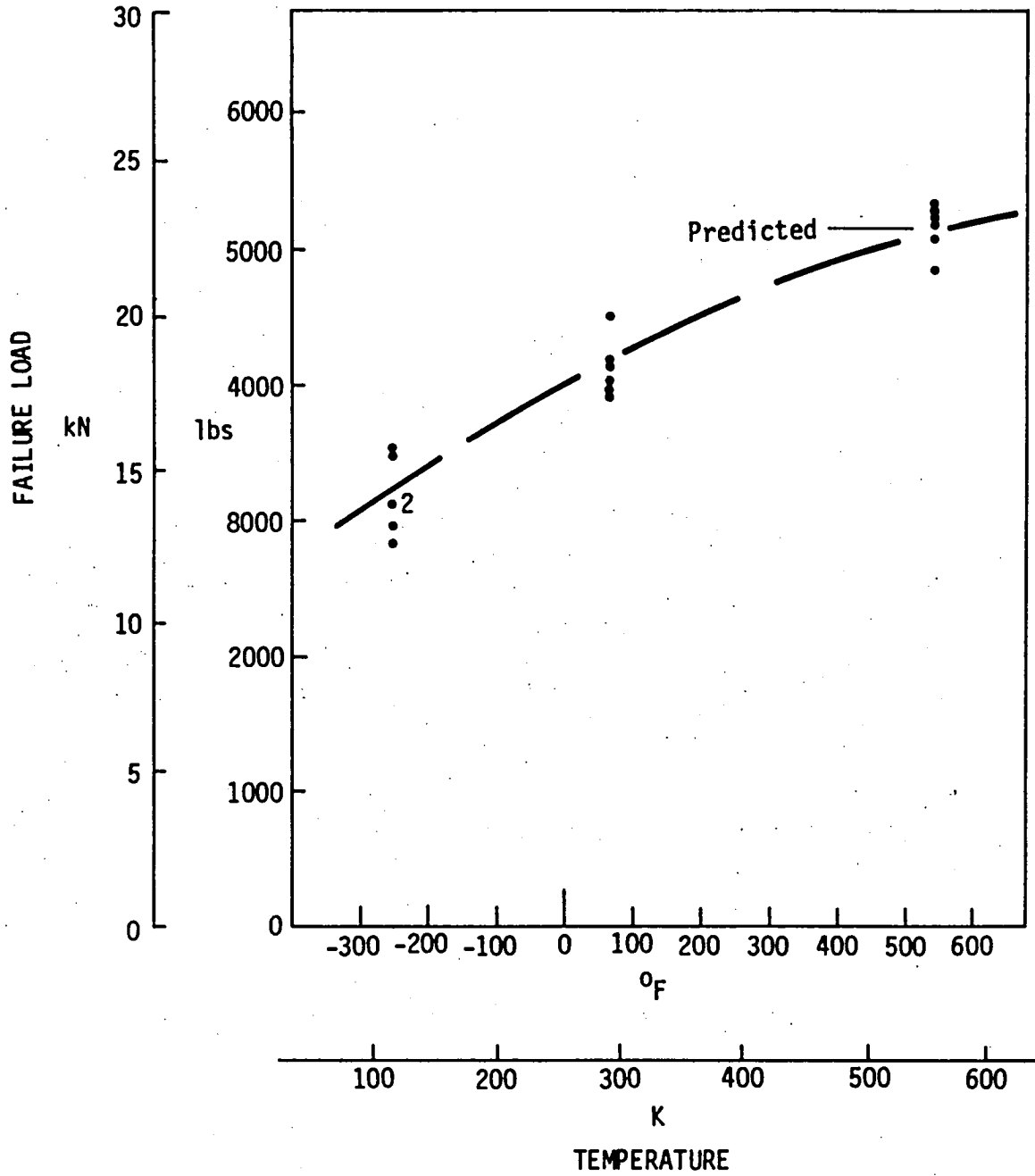


Figure 3-21 Matrix 3G Test 1a - 3 Step Sym. Step-Lap Joint, Aged, GR/PI to Titanium

SECTION 4.0

CONCLUDING REMARKS

During this reporting period the principal program activities dealt with design of static discriminator test specimens, and testing of "Net Tension", "Thick Adherend", "Standard Joint", "Small Specimen", and "Integral Doubler" specimens.

Results of testing discussed in this report have led to the following conclusions:

- o Integral (co-cured) doublers are stronger than bonded doublers.
- o For the joint configurations tested, the A7F adhesive is stronger than the GR/PI laminate.
- o Bonded double lap joints are more efficient than single lap joints.

REFERENCES

1. "Comparison of Theoretical and Experimental Shear Stress in the Adhesive Layer of a Lap Joint Model", William W. Sharpe, Jr., Theodore J. Muha, Jr., 1974 Army Symposium.
2. NASA Technical Memorandum 81796, "Effects of Method of Loading and Specimen Configuration on Compressive Strength of Graphite/Epoxy Composite Materials", Ronald K. Clark and W. Barry Lisagor, April 1980.
3. "Primary Adhesively Bonded Structure Technology (PABST) Design Handbook for Adhesive Bonding", AFFDL-TR-79-3129, November 1979.
4. Arnquist, J. L. and Skoumal, D. E., "Design, Fabrication and Test of Graphite/Polyimide Joints and Attachments for Advanced Aerospace Vehicles", Quarterly Progress Report #3, Contract NAS1-15644, NASA CR-159110, October 15, 1979.





